

NASA Contractor Report 3842

RF Characteristics of the Hoop Column Antenna for the Land Mobile Satellite System Mission

Peter Foldes

Foldes Incorporated

Wayne, Pennsylvania

Prepared for
Langley Research Center
under Contract NAS1-17209



National Aeronautics
and Space Administration

Scientific and Technical
Information Branch

1984

TABLE OF CONTENTS

1.	INTRODUCTION	1
2.	REQUIREMENTS FOR LAND MOBILE SATELLITE SYSTEM	2
3.	DEVELOPMENT OF BEAM TOPOLOGY PLAN	18
4.	ANTENNA GEOMETRY	23
5.	RADIATION CHARACTERISTICS FOR VARIOUS FEED IMPLEMENTATIONS	33
6.	FEED CONFIGURATION ALTERNATIVES	48
7.	S-BAND SUBSYSTEM	54
8.	CONCLUSIONS AND RECOMMENDATIONS	60

1. INTRODUCTION

The advent of the Space Transportation System (STS), as an operational vehicle, has made it possible to use larger and heavier structures in future space applications.

With this potential in mind, a Large Space System Technology (LSST) program was established by the NASA at the Langley Research Center with the objective of conducting both in-house and industry studies into the theoretical and experimental implementation problems associated with large space structures.

A wide range of missions requiring large space structures has been proposed, and specific systems are now being reviewed in more detail to allow the continuation of the LSS technology development. Specifically, a land mobile communications system, a soil moisture measuring radiometer system, and a very large base interferometer system have been given much attention. Contrary to the present trend, where communication satellites are utilizing ever higher radio frequencies (15 GHz to 60 GHz), these missions require relatively low radio frequencies (0.86 GHz to 1.4 GHz). Antenna diameters are in the 30-meter to 150-meter range.

Historically, communications systems have provided the most important commercial utilization of space. For this reason, an advanced mobile communications mission was adjudged to be the most likely candidate for a large space structure application. With that in mind, it was decided to concentrate a large part of the 1981 LSST technical development activity toward the definition of a spacecraft for the Land Mobile Satellite System (LMSS).

These activities were conducted under the auspices of the LSST program office at the LaRC with the participation of the LaRC, LeRC, and JPL and several aerospace firms.

Recognizing that a spacecraft configuration for the LMSS will be dominated by the requirements imposed by the reflecting antenna system because of its size, weight, accuracy, alignment, and control, more detailed investigations of different antenna systems were initiated. One antenna configuration was based on a 55-meter diameter offset-fed parabolic reflector utilizing Lockheed's wrap-rib deployment concept and a multiple beam feed developed by JPL. Another configuration was based on an approximately 120-meter diameter structure utilizing four offset fed apertures employing a quad aperture, hoop column antenna deployment concept being developed for the LaRC by the Harris Corporation. The multiple-beam feed conceptual design for the quad aperture antenna was conducted by the General Electric Company (under contract (NAS1-16312)

This report presents the results of the RF definition work for the quad aperture antenna. The elements of the study requirements for the LMSS system will be summarized, followed by the development of a beam topology plan which satisfies the mission requirement with a practical and realizable configuration. Based on this topology, the geometry of the UHF antenna, which is used for direct links to and from the mobile users, and its radiation characteristics are defined. This is followed by a discussion of the various feed alternatives. The next section discusses the S-band aperture used for the links with fixed base stations. Finally, the report contains a conclusion and recommendation section.

2. REQUIREMENTS FOR THE LAND MOBILE SATELLITE SYSTEM

As mentioned previously, a number of missions were identified as being likely beneficiaries of a large space structures development effort. Of these, the Land Mobile Satellite System (LMSS) was considered to be the most urgent and as such was selected as a point design for the 1981 LSST development effort.

The need for the LMSS has been recognized for many years, and its system requirements given considerable attention (refs. 1 and 2).

There are approximately 300 million telephones in the United States, each capable of interconnection between subscribers. However, access to this vast network from a mobile telephone is limited by the available frequency bands to 140,000 subscribers. In addition, when a channel is available, the present cost (approximately \$150 per month) is a strong deterrent to most potential users.

To alleviate this situation, the telephone companies are planning to install a ground-based mobile communication system. When fully operational about 1995, this system will provide high quality telephone communications for millions of users in metropolitan areas and along major highways. The overall service will be divided into cells, giving rise to the name "Cellular System" to describe the operation. The mobile user will communicate in the 806 MHz to 890 MHz radio frequency band to a base station placed on a high tower to give good line of sight visibility. The base station provides access to the fixed telephone network.

In principle, a land-based cellular system can cover the continental United States, but because it is neither economical nor practical to provide the necessary towers and base station equipment for sparsely populated areas, the need exists for an additional system to augment the cellular. It is assumed that this complimentary system is satellite based, as it appears to be the only competitive alternative at the present time.

Before the requirements for such a system can be established, the following basic questions must be resolved:

1. What is a reasonable time frame for full implementation?
2. What is the expected satellite lifetime?

3. How many subscribers can be anticipated?
4. Should the augmenting system be compatible with the cellular system?
5. What quality is acceptable?

Definitive answers to these questions require a very detailed system analysis beyond the scope of this report, but on the basis of previous studies and the consensus of the investigators forming the present study team, a set of preliminary requirements was established. These requirements are summarized in tables 2.1 to 2.5. The following remarks are presented to give some clarification to the rationale leading to answers to questions 1 to 5 above.

The start of operation is determined by the time necessary to develop the required spacecraft technology and an economical network of land mobile equipment. Considering the complexity of the spacecraft, the extent of the ground equipment necessary and limited budgeting, 10 to 12 years seems reasonable. This places the desired operational ready time to be about 1995.

The assumed lifetime (10 years) is slightly longer than most present day satellites, but if it can be achieved, it is a practical way to reduce operational costs.

TABLE 2.1.- ASSUMED REQUIREMENTS FOR THE OVERALL SYSTEM
AND LAUNCH VEHICLE

Overall system

Start of operation	1995
Lifetime	10 years
Maximum user capacity (nominal)	250,000
Blocking probability	p = 0.02
Distribution of users:	
Initial	Uniform (without VOX)
Eventual	Population density related (with VOX)
Compatibility with ATT cellular system:	
Initial	Yes
Eventual	Not with present cellular system
Eclipse capability	20 percent
Transponder type	Nonswitching (bentpipe)
Orbit	Geosynchronous 110° long
Nominal slant range	R = 36,800 km
Polarization	CP
Coverage area	U.S. 48 states
Pointing accuracy	0.03° peak

Launch vehicle

Earth to Leo	STS
Leo to Geo	TBD*

*Potential vehicle may provide following geo payload limits:
6350 kg/9.75 m to 4082 kg/12.76 m.

The number of eventual users has a major impact on the design of the spacecraft, and particularly of the antenna. This number cannot be exactly determined at this time, but an idea of its upper limit can be estimated. If the metropolitan areas with populations over 200,000 are eliminated from the service area on the basis that they will be served by the telephone companies' cellular system, a residual population of 44 million remains. Assuming only 5 percent of this number, 2.2 million are potential users who cannot be connected to the cellular system, an LMSS with 250,000 user capacity does not seem unrealistic.

It is assumed that the 250,000 users are evenly distributed. A maximum of 110,000 users could be attained in more populous areas, though this could

be extended by reducing the required bandwidth per channel and increasing the radiated EIRP.

An important point to be considered concerns the degree of compatibility between the LMSS and the cellular system. Obviously, full compatibility is a desirable goal. But even if the basic characteristics of the satellite link (frequency band, channels, modulation techniques, etc.) are made identical, other factors such as propagation variables, man-made noise, and rural service quality, would have a detrimental affect. For this reason, it is assumed that the initial LMSS will be made as compatible as possible, but with the understanding that some deviation is permissible to allow for contingencies.

The aim of achieving compatibility, and the desire to keep the spacecraft payload as simple as possible, dictates the use of a nonswitching, or bent pipe, transponder. In this configuration, two radio frequency bands, UHF and S-band, are used for the complete connection. The mobile user communicates with the satellite over the UHF links. The satellite connects the user, through the base station, to and from the fixed telephone subscriber via the S-band links. All circuit switching is performed on the ground.

The size and weight of the spacecraft is mainly dependent on the antenna and power system, which in turn are functions of the required telecommunications capacity. To minimize the power system requirements, only a 20 percent eclipse capability is assumed. This should have little affect on service, since vehicle traffic, and hence mobile communications, falls off rapidly at night.

The position of the satellite in geo-synchronous orbit has been established at 110° west longitude. This assures the largest possible elevation angle for mobile users in the contiguous states, and the smallest possible average service area per beam cell. In the contiguous states, elevation angles range from a high of 54° at Corpus Christi, Texas, to a low of 24° at

Bangor, Maine. The elevation angle at Honolulu, Hawaii, is 31°. The lowest, of course, is found at Alaska's north slope, where it is only 5°. However, Fairbanks, Alaska, has an elevation angle of 11°.

The choice of 110° west longitude means that eclipse takes place at 11:00 p.m. local time in the Pacific time zone, and 2:00 a.m. local time in the Eastern time zone, allowing battery weights to be kept to a minimum. It may be noted that a slight overall capacity is possible by favoring the Eastern time zone using a satellite longitude of 78°, but only at the expense of losing coverage for some parts of Alaska, and increasing the weight of batteries.

The frequency assignments for the system (shown in table 2.2) utilize the UHF band for the up and down links between mobile users and satellite, and the S-band links for the up and down links between the base stations and satellite. The base station connects the mobile user to the fixed subscriber through the existing telephone network.

TABLE 2.2.- FREQUENCY ASSIGNMENTS FOR LMSS

Mobile to satellite	821 to 831 MHz
Satellite to base station	2550 to 2590 MHz
Base station to satellite	2650 to 2690 MHz
Satellite to mobile	866 to 876 MHz
Maximum audio frequency	$B_A = 3.4$ KHz
IF noise bandwidth	$B_{IF} = 25$ KHz
Carrier separation	$B_O = 30$ KHz
Allocation band subdivision	$K = 4$
UHF bandwidth per beam	$B_{BU} = 2.5$ MHz
S-band bandwidth per beam	$B_{BS} = 10$ MHz
UHF channels per beam	$M_U = B_{BU}/B_O = 83$
UHF voice channels per beam	$V_U = 81$
UHF signaling channels per beam	$S_U = 2$
S-band channels per beam	$M_S = 332$
S-band voice channels per beam	$V_S = 324$
S-band signaling channels per beam	$S_S = 8$
Channel designations, UHF	
Set 1	1, 5, ..., 329
Set 2	2, 6, ..., 330
Set 3	3, 7, ..., 331
Set 4	4, 8, ..., 332

It is assumed that a 10 MHz bandwidth is available for both the UHF uplink (821-831 MHz) and downlink (866-876 MHz), and that these bands are not shared with other communication systems. For the S-band links, 40 MHz bandwidths are assumed. The communication format is compatible with AT&T's contemplated cellular system, since the mobile communication system provides a service for those remote users who cannot be served economically by the land-based cellular system.

The selected frequency bands are compatible with the WARC 79 assignments for mobile radio in the UHF and S-bands. Of the 84 MHz bandwidth of the UHF band (806-890 MHz), 20 MHz are assumed for the satellite service. This is 23.8 percent of the total. As mentioned earlier, the unserved population was 44 million, or 19.1 percent of the total. Thus, the share of the spectrum is roughly equivalent to the share of the population to be covered.

In order to provide the required number of user channels, the 10 MHz uplink and downlink spectra must be utilized repeatedly. This is achieved by dividing the total coverage into a large number of cells and reusing a spectrum in those cells, somewhat analogous to the ground-based cellular system. However, whereas the ground-based cellular system obtains isolation between identical frequency band cells by spatial separation (signal attenuation), isolation in the satellite system must be provided by proper sidelobe levels of the multibeam antenna. It can be shown that for the required isolation, the complexity, and spectrum efficient use of the spacecraft antenna is acceptable if the 10 MHz allocated spectrum is divided into four sub-bands.

These sub-bands can be unequal for better matching of the traffic distribution, but in the following discussion they are assumed equal for simplicity. This gives a UHF bandwidth per beam (B_{BU}) of 2.5 MHz. For compatibility with

the cellular system, a voice carrier separation frequency (B_0) of 30 KHz is required. This allows 83 standard voice channels per beam. If two channels are reserved for signalling, 81 channels remain for voice traffic. With a four frequency split, these 81 channels are equivalent to $81 \times 4 = 324$ usable voice channels or $324 \times 30 = 9720$ kc. Allowing a blocking factor of 0.02 gives a total of $9525 \div 3.4 = 2800$ voice circuits, or $2800 \div 83 = 33$ users per channel.

The above plan allows for $4 \times 83 = 332$ standard UHF voice channels. There are several ways in which these channels can be divided into four non-interfering sets. The grouping shown in table 2.2 (set #1 formed from channels 1, 5, 9, ..., 329, set #2 from channels 2, 6, 10, ..., 330, etc.) has the advantage of easier channel filtering and identical total RF band for all beams.

Table 2.3 gives the basic characteristics of the beam topologies and the required EIRP's and G/T's. To service approximately one quarter million subscribers, 91 UHF beams (cells) were selected to cover the 48 contiguous states ($U_0 = 91 \times 2673 = 243,607$ users). This means a UHF beamwidth (cell size) of $\alpha_u = 0.423^\circ$. The corresponding numbers at S-band are 23 cells with $\alpha_s = 1.0^\circ$. Adequate isolation between cells using the same frequency and polarization is achieved by dividing the 10 MHz band into four sub-bands and using two polarizations, giving in effect eight independent, practically "orthogonal" sub-bands. The topology plan is arranged in such a way that one cell separates two cells sharing the same frequency but having different polarizations, and two cells separate two cells sharing the same frequency and polarization. The number of users referred to above, 243,607, assumes a uniform distribution. If population density becomes a factor, the number of users drops to 106,943.

TABLE 2.3.- BEAM TOPOLOGY AND EIRP CHARACTERISTICS FOR THE LMSS SYSTEM

Cell size, UHF	$\alpha_U = 0.423^\circ$
Cell size, S-band	$\alpha_S = 1^\circ$
Number of cells, UHF	$N_U = 91$
Number of cells, S-band	$N_S = 23$
Total number of channels	$T_C = N_U M_U = 7553$
Total number of voice channels	$T_V = 7371$
User per channel for $V_U = 81$	33.05
Users per beam	$U = 2677$
Users in total system	
Uniform distribution	$U_O = UN_U = 243,607$
Population density related distribution	$U_M = 0.439 U_O = 106,943$
Typical EW cell width	$D_C = 272 \text{ km}$
Typical cell area	$A_C = 82,000 \text{ km}^2$
Area per user (uniform distribution)	$A_U = 30.6 \text{ km}^2$
Average distance between users	$\lambda_U = 5.53 \text{ km}$
Number of EW cells (UHF)	15.5
Number of NS cells (UHF)	7.8

	<u>UHF</u>		<u>S-Band</u>	
	<u>Up</u>	<u>Down</u>	<u>Up</u>	<u>Down</u>
f (MHz)	821	866	2650	2550
λ (m)	0.3654	0.3464	0.1132	0.1176
Ground EIRP, dBW	12		20.6	
Ground G/T, dB		-24.5		16.2
Space EIRP, dBW	42.3 (at contour)			20 (at peak)
Space G/T, dB	22.2		8.8	

It must be emphasized that even though the above topology plan utilizes orthogonal polarization it does not do so in the same cell. This requires a modest polarization isolation because the beam isolation by itself is insufficient to provide the total required.

There is some question that this modest isolation (axial ratio) can be achieved for the mobile antenna under extreme propagation conditions without some form of automatic polarization tracking capability.

The advantage of dual polarization can be demonstrated by the following example. If only one polarization is used, the 10 MHz bandwidth must be divided into a minimum of seven sub-bands to give comparable, but slightly

poorer isolation. In this case only 47 channels (46 voice channels) are available per beam. The end result is 30.8 users per channel or 1474 users per beam, compared to 2677 users per beam in the dual polarization configuration. This is a drop in capacity of 47 percent.

It is interesting to note that with the four frequency, dual polarization plan, the average distance between subscribers is 5.53 km.

Table 2.3 also gives the assumed EIRP and G/T for the UHF and S-band systems. These values are compatible with the selected cell sizes, mobile equipment capability, and overall performance requirements. (A typical link analysis will be given later.)

Table 2.4 summarizes some of the electrical and mechanical characteristics of the spacecraft and ground terminal UHF equipment. For the spacecraft antenna a hoop-column structure is assumed with the main disk divided into four sub-apertures (quad-aperture configuration). This approach maintains an axially symmetrical overall antenna structure; at the same time, the central blockage associated with the bulky feed necessary for multibeam operation is eliminated. This is accomplished by utilizing only part of the four quadrants of the available overall reflector surface. In this configuration, the total required diameter is a little more than twice the diameter of a single sub-aperture. However, the availability of four sub-apertures makes it possible to incorporate a number of system simplifications and to enhance the performance.

TABLE 2.4.- FRONT END CHARACTERISTICS OF THE LMSS IN UHF BAND

UHF, downlink, spacecraft

Antenna type	Hoop column, quad-apertures
Overall diameter	$D_o = 118 \text{ m}$
Sub-aperture diameter average	$D_{av}^d = 53 \text{ m}$
Sub-aperture major/minor axes	55 m/51 m
Offset	$Q = 0.111 D_{av}^d$
Focal length	$F = 66 \text{ m}$
Feed diameter	$D = 0.553 \text{ m}$
Sub-aperture utilization	East/West
Maximum scan	$\theta_M/\alpha_V = 3.5$
Loss less peak gain for maximum scan	$G_{MO} = 48.5 \text{ dB}$
Contour gain differential	$\Delta G = -2.5$
Circuit loss	$\alpha_L = 0.2 \text{ dB}$
Minimum gain	$G = 45.8 \text{ dB}$
Transmit power per voice channel	$P_{TU} = -4 \text{ dBW} = 0.4 \text{ W}$
Transmit power per beam	$P_{TU_b} = 33.2 \text{ W}$
Total transmit power	$P_U = 3021 \text{ W}$
Transmitter efficiency	$\eta_U = 50 \text{ percent}$
DC power for transmitters	$P_{OU} = 6042 \text{ W}$
Beam isolation	$I = 25 \text{ dB}$
Intermodulation	$IM = 25 \text{ dB}$
Polarization	RCP or LCP
Axial ratio	0.5 dB

UHF, downlink, Earth station

Antenna type	Crossed dipole over ground plate (Quantity - 2 for diversity)
Polarization	Selectable RCP or LCP
Axial ratio	5 dB
Antenna receive area	$A_R = 0.015 \text{ m}^2 = -18 \text{ dB/m}^2$
Receiver noise temperature (with 2 low noise front end)	$T_R = 26 \text{ dB/}^\circ\text{K}$
G/T	-24.5 dB/°K

There are a number of ways multiple apertures can be utilized to introduce certain system advantages. Table 2.5 summarizes the most important configurations possible with two or four sub-apertures.

TABLE 2.5.- POSSIBLE FUNCTIONS WITH MULTIPLE SUB-APERTURES

Case	No. of sub-apertures	Functions	Advantages
A	2	Uplink - downlink	Single band feed, no diplexer
B	2	East - West	Minimum scan effect
C	2	RCP - LCP	Single polarized radiating element
D	2	Heavy traffic - thin traffic	Matching nonuniform traffic distribution
E	4	Channel 1,2,3,4	Allows large feed with simple BFN
F	4	A + B	
G	4	A + C	
H	4	A + D	
I	4	B + C	
J	4	B + D	
K	4	C + D	

The utilization of two sub-apertures is quite common. Most present-day communication satellite antennas are based on case A, which separates the uplinks and downlinks and thereby allows the antenna design to have relatively narrow bandwidth and eliminates the need for the transmit-receive signal combining diplexer.

Case B is advantageous when the overall coverage area is elongated, like CONUS. By dividing the area into two (East and West group of the 48 states) the subcoverage area shapes are closer to axial symmetry; thus the gain and sidelobe deterioration associated with the scan of the component beams is minimized. This reduces the power requirement of the system, improves the beam isolation, or, for constant beam isolation, allows a reduction of focal distance.

Case C allows the utilization of singular polarized radiating elements, thus eliminating orthogonal couplers, or allowing other simplifications in the polarizing circuitry of the feed. Additionally, it allows coincident beam maximums for the RCP and LCP component beams, which is not possible with single, dual polarized elements.

Case D separates the heavy route and thin route traffic by using different sub-apertures. In typical system configurations these types of traffic are separated into different parts of the overall allocation bandwidth, and the heavy route areas are superimposed on the thin route areas. When a common sub-aperture is used to handle such traffic, the bands must be combined in the radiating elements by diplexers. Case D eliminates the need of diplexers.

Case E provides a separate sub-aperture for each RF frequency band in a four frequency plan configuration. This allows one "empty" cell between identical frequency band component beams; thus the diameter of the radiating elements can be increased by about 83 percent relative to the single aperture case. The resulting larger edge-taper yields a beam isolation approaching the one with the seven element (overlapping) feed, but it maintains feed simplicity.

Case E and the possible combinations of cases A through D define a total of seven practical, interesting cases for the utilization of a quad-aperture antenna.

For the present design separate sub-apertures are used for the uplink and downlink, which eliminates the need of receive/transmit diplexers. Additionally, the East and West part of the country is served by separate sub-apertures, which reduce the scan requirement of the component beams.

On the basis of the selected aperture functions the nominal geometry of the antenna and its main electrical characteristics can be determined. These

are shown in table 2.4. The most important of these characteristics are the sub-aperture diameter of 53 m and the associated overall antenna diameter of 118 m. The sub-aperture diameter is necessary to provide 91 beams over CONUS with the required 25 dB beam isolation in the UHF band. It is assumed that for such a reflector geometry, a seven-element feed is necessary to provide the desired isolation, resulting in a peak downlink gain for the maximally scanned beam of 48.5 dB, and a minimum contour gain of 45.8 dB.

According to the link budget calculations, such an antenna gain with 0.4 watt per voice channel PA power, gives a carrier to total noise ratio of 17.7 dB, which provides nearly 8 dB fading margin. The transmit power per beam is 33.2 watts (83×0.4) producing a total UHF radiated power of 3021 watts (91×33.2).

There is a major assumption about the quality of the transmitters in table 2.4 which is beyond the current state of art. This is the feasibility of the simultaneously achieving 50 percent DC to RF conversion efficiency, and -25 dB intermodulation distortion. With this assumption, 6042 watt dc power is necessary to maintain the UHF system. Present state of art is closer to 25 percent efficiency for the above conditions. If the predicted improvement of the PA state of art cannot be fully realized within the stipulated time frame, then either an increased power source or lower fading margin, or a combination of the two must be accepted.

Relatively modest performance characteristics are assumed for the ground mobile equipment. The antenna itself provides 0.015 m^2 effective receive area (achievable by a crossed dipole over a ground plane) and two such units are provided for diversity similar to the cellular system. However, two differences were assumed: the antennas will be circularly polarized (switchable to

RCP or LCP) and the front end of the receiver will be directly at the output of the antenna. This may represent a modest cost increase for the rural user.

Table 2.6 gives the front end characteristics of the S-band subsystem. A relatively small, 7.7 m offset fed paraboloid antenna is selected for this subsystem in order to simplify its deployment and allow its mounting behind the UHF feed.

TABLE 2.6.- FRONT END CHARACTERISTICS OF THE LMSS IN S-BAND

S-band, downlink, spacecraft	
Antenna type	Offset fed sub-aperture common for E/W and up/down. Mounted on back of UHF feed.
Antenna diameter	$D_S = 7.7$ m
Focal length	$F = 7.7$ m
Maximum antenna gain	$G_{SM} = 42.8$ dB
Minimum antenna gain	$G_{SM} = 39.3$ dB
S-band, downlink, Earth station	
Antenna type	Symmetrical Cassegrain
Antenna diameter	4.5 m
Antenna gain	44 dB
System noise temperature	$150^\circ\text{K} = 21.8$ dB/ $^\circ\text{K}$
G/T	11.1 dB/ $^\circ\text{K}$

The diameter of the S-band antenna has an effect on the total required S-band spectrum, and the average distance between S-band base stations. This in turn affects the cost of the long distance land line connections.

The selected antenna diameter required 2×40 MHz S-band spectrum space and assumes 180 km average distance for the land line between S-band base station and fixed user. While an increased antenna diameter would reduce both of these figures, the saving in ground costs would probably be offset by the increased spacecraft complexity.

On the basis of the previously discussed assumptions the carrier to noise ratios for the various communication links can be calculated. Because the UHF downlink has the largest significance, this link is used to illustrate the calculations given below.

For $R = 36,800$ km

$$\alpha_{\text{Link}} = \frac{1}{4\pi R^2} = -162.3 \text{ dB/m}^2$$

$$P_{\text{TU}} = -4 \text{ dBW}$$

$$G = 45.8 \text{ dB}$$

$$A_{\text{R}} = -18 \text{ dB}$$

$$\begin{aligned} \text{Carrier, } C &= (\alpha_{\text{Link}} + P_{\text{TU}} + G + A_{\text{R}}) \text{ dBW} \\ &= (-162.3 - 4 + 45.8 - 18.2) \text{ dBW} = -138.5 \text{ dBW} \end{aligned}$$

For $k = 228.6$ dBHz/W

$$T = 26.5 \text{ dB/}^\circ\text{K}$$

$$B_{\text{C}} = 25 \text{ kHz} = 44 \text{ dB/Hz}$$

$$\begin{aligned} \text{Thermal noise, } N_{\text{T}} &= (k + T + B_{\text{C}}) \text{ dBW} \\ &= (-228.6 + 26.5 + 44) \text{ dBW} = -158.1 \text{ dBW} \end{aligned}$$

$$\left(\frac{C}{N_{\text{T}}}\right)_{\text{RF}} = 19.6 \text{ dB} \quad \frac{C}{N_{\text{T}_0}} = 63.6 \text{ dB/Hz}$$

For $\frac{C}{I} = 25 \text{ dB}$, $\frac{C}{\text{IM}} = 25 \text{ dB}$

$$\left(\frac{C}{N}\right)_{\text{RF}} = \frac{C}{N_{\text{T}} + I + \text{IM}_{\text{RF}}} = 18 \text{ dB}$$

With uplink caused degradation allowance of 0.3 dB

$$\left(\frac{C}{N}\right)_{\text{RF}} = 17.7 \text{ dB} \quad \text{Margin} \sim 7.7 \text{ dB}$$

FM improvement	11.3 dB
De-emphasis improvement	7.5 dB
Subjective expander improvement	11.0 dB
Message weighting	<u>2.0 dB</u>
Total processing improvement	31.8 dB

The following pages contain a more detailed analysis of the possible approaches that can be taken to justify the assumptions and realize the above requirements.

3. DEVELOPMENT OF BEAM TOPOLOGY PLAN

The beam topology plan is designed to make optimum use of frequency and polarization assignments for the cells covering the overall service area.

Since the present requirement is for a contiguous coverage system, subdivision of the 10 MHz frequency band is inevitable. While the beam isolation problem decreases with increasing subdivision, at the same time the traffic handling capacity decreases. For the presently required 25 dB minimum beam isolation, the necessary number of subdivisions are seven or eight. These can be realized by seven single polarized channels or four dual polarized channels. As was discussed previously, the four-frequency, dual-polarized channel alternative was selected because it provides the most efficient use of the spectrum.

Figure 3.1 shows the beam topology plan for uniform user distribution. The actually developed conceptual design for the feed is for the uniform distribution, but the East West subdivision and the panelization of the feed required for launch packaging takes the potential density distribution boundary lines into account. Within the overall feed topology plan the numbers in the cells show the subfrequency band (RF channel) numbers assigned for a cell.

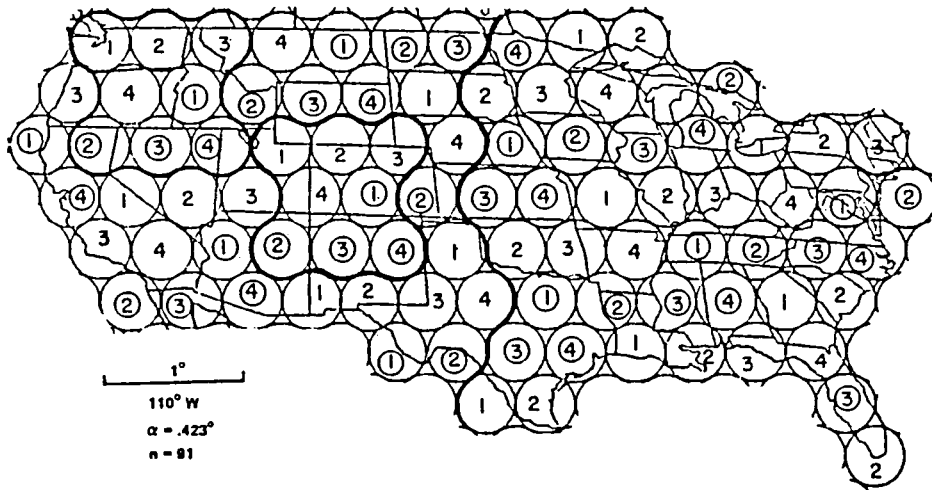


Figure 3.1.- Beam topology plan for uniform user density distribution.

Uncircled and circled numbers represent orthogonal polarizations. Eight cells, like 1,2,3,4, ①, ②, ③, ④ form a "grand cell" (shown by heavy boundary) which can be repeated indefinitely. As shown in figure 3.1, a cell carrying subchannel ① is always separated by two cells from another cell carrying channel ①. The same applies to a cell carrying channel 1, which is separated by two cells from another cell carrying channel 1.

The feed array elements (sub-arrays) corresponding to this topology plan have a similar layout. When such a feed is divided along an approximately N-S line, shown by heavy boundary into two assemblies, "East" and "West," then the boundary located feed providing coverage ① generally must utilize more than one radiating element for control of its sidelobes, to minimize pickup by the other No. ① cells. To accomplish this the "East" and "West" feeds are made to overlap.

The plan shown in figure 3.1 assumes uniform user distribution. This allows a maximum of 2677 users per beam. When this number is first reached in a given cell (presumably in the most heavily populated areas) the traffic

cannot be expanded. At the same time, other parts of the system may be operating much below capacity.

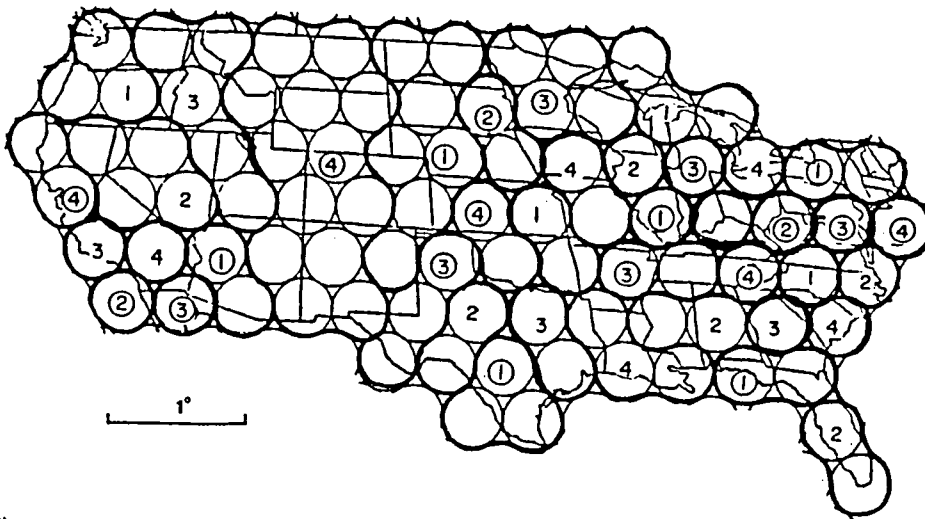
This problem can be alleviated in a number of ways, as follows:

- (a) Increasing the coverage of the ground-based cellular system.
- (b) Dividing the 10 MHz bandwidth into unequal sub-bands.
- (c) Combining some cells into larger areas to give greater coverage.
- (d) Superimpose heavy route, and thin route traffic areas, with different bandwidth assignments.

The implementation of case (a) and (b) does not require any change in the satellite. (c) or (d) require some reconfiguration in the satellite antenna, or some modification of the original design relative to the above discussed uniform distribution case.

Figure 3.2 is a simplification of the plan given in figure 3.1. This plan takes into account that the users are not distributed uniformly over the area of the 48 states. The simplification results in 40 available beams and a user capacity of only 43.9 percent of the original. However, if this plan is combined with the use of Voice Operated Transmitters (VOX), approximately 71.6 percent of the original users (uniform user distribution, no VOX) can be achieved.

Note that if the plan shown in figure 3.2 is adopted the maintenance of the original EIRP requires the same total power. For example, the large beam covering the Rocky Mountain area, using sub-band four, requires 13 component beams, thus has 13 times less gain. In order to maintain the same EIRP its associated transmitter must radiate 13 times higher power, giving the same power per component beam as previously. However, a number of previously used frequency bands become available for use in heavier traffic cells. For example, in the cell covering Los Angeles, in addition to the assigned



110° W
 $\alpha = .423^\circ$
 $n = 91$
 $n_b = 40$
 $\frac{n_b}{n} = .439$

WITH VOX AND SAME POWER
 AS FOR UNIFORM DISTRIBUTION
 .716 OF ORIGINAL USERS (174 685)
 CAN BE ACCOMMODATED

Figure 3.2.- Beam topology plan for nonuniform user density distribution.

channel 2, use can be made of channel 1, thus doubling the capacity. The associated satellite "reconfiguration" simply involves the use of all the indicated cells in the designated frequency band and polarization.

The beam topology plans exhibited in figures 3.1 and 3.2 assume only one mobile communication system in the given frequency band, since practically no antenna directivity can be expected for the mobile user. This means that when mobile communication systems are extended beyond CONUS into Canada and Mexico, these systems (in the same frequency band) must be compatible with the beam topology plan of the CONUS system. (Compatibility means cell size, channelization and polarization assignment.)

Figure 3.3 shows the extension of the beam topology plan exhibited in figure 1 to cover the North American continent. The overall plan provides 91 singlet beams coverage for the U.S. and 31 beams each for Canada and Mexico. The plan allows seven-element feeds for the formation of all U.S. cells and

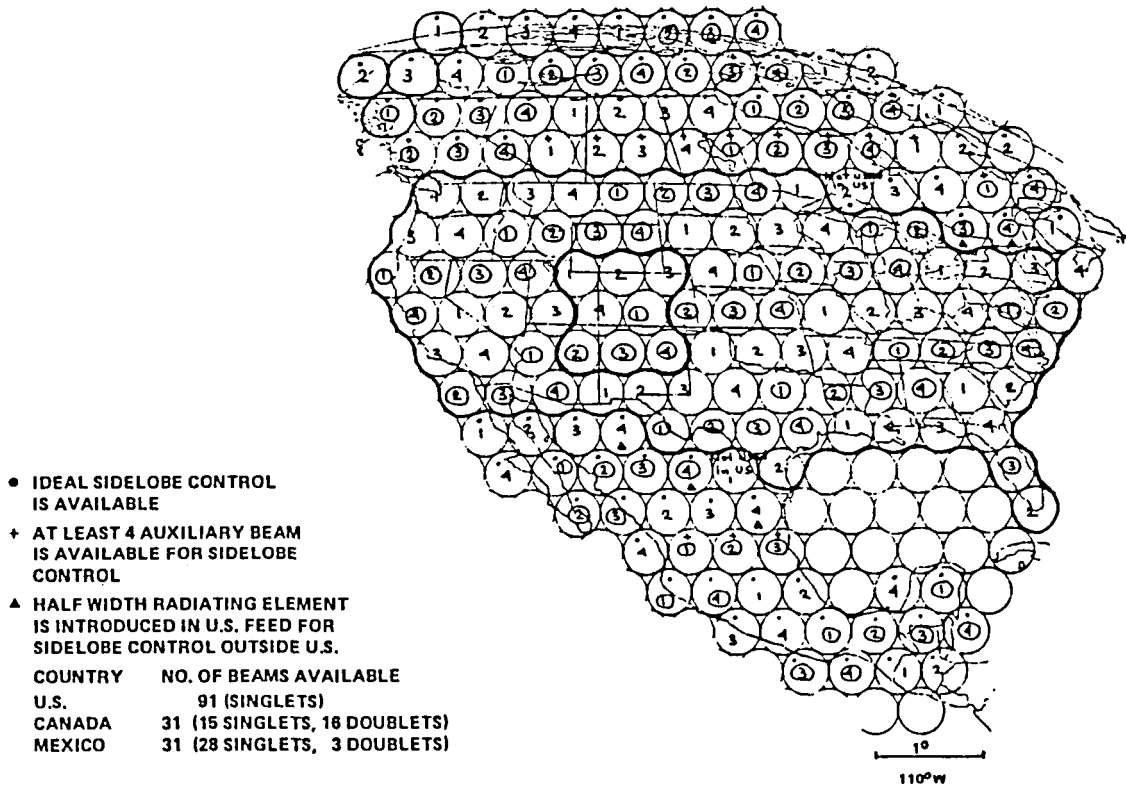


Figure 3.3.- Extension of the beam topology plan over the North American continent.

for those Canadian and Mexican cells which are marked by a dot. The seven-element feed configuration allows ideal sidelobe control for the beams associated with the corresponding cells. When the feed array associated with U.S. coverage is extended beyond the indicated heavy boundary by at least five (half width) radiating elements for the cells marked by Δ , the sidelobe level is controlled by four auxiliary beams for those Canadian and Mexican cells which are marked by +. This allows at least 25 dB beam isolation anywhere within the North American continent using the above beam topology plan.

4. ANTENNA GEOMETRY

The conceptual geometry of the quad antenna is determined by the basic structural and deployment concept of the hoop-column configuration. The rigidity of this structure is based on an axially symmetrical toroidal hoop which is stressed against a column by a set of guywires. In such a configuration the feed must be close to the axis of symmetry where the feed, the column, and the guywires cause blockage and scatter.

The detrimental side effects can be reduced to an acceptable level if the overall aperture of the antenna is broken down to at least two sub-apertures allowing the elimination of the feed blockage. Some column and wire scatter remains, but this can be made small compared to the feed blockage effect resulting from a single, symmetrical aperture. The price for the elimination of blockage of course is large, more than a factor of two reduction of the available minimum aperture diameter. However, for many situations this loss is compensated for by the advantages gained by the use of multiple apertures.

For the present application the overall aperture is divided into four sub-apertures, hence the name "Quad Antenna." In comparison of two, three, and four way division of the overall aperture of the hoop-column structure the four way division gives practically the same minimum sub-aperture diameter as the two or three way division, but gives the largest number of sub-apertures with reasonable utilization of the overall aperture.

In the simplest possible case the four sub-aperture diameters are equal. For this situation, the uplink and downlink antenna gains are about equal. In practice, it is advantageous to increase the downlink antenna gain at the expense of the uplink antenna gain and achieve a saving in the satellite transmit power required, to the benefit of the mobile user. Unequal uplink and downlink sub-aperture sizes create a gap in the aperture plane

projections of the uplink sub-aperture and its corresponding feed. This gap can be utilized to emplace solar arrays in a nonscattering locale. When downlink sub-apertures are in the vicinity of the NS plane the possible downlink sub-aperture is the largest, but the solar arrays must be in the EW plane and would require a two-axis gimbal for sun tracking. When the downlink sub-apertures are in the EW plane the solar arrays are in their conventional NS location relative to the feed (spacecraft); thus a single-axis rotator is adequate for their operation. Both of these solutions have their own merits.

Figure 4.1 shows the front view geometry of the quad antenna, which is compatible with the system requirements and the beam topology plan discussed

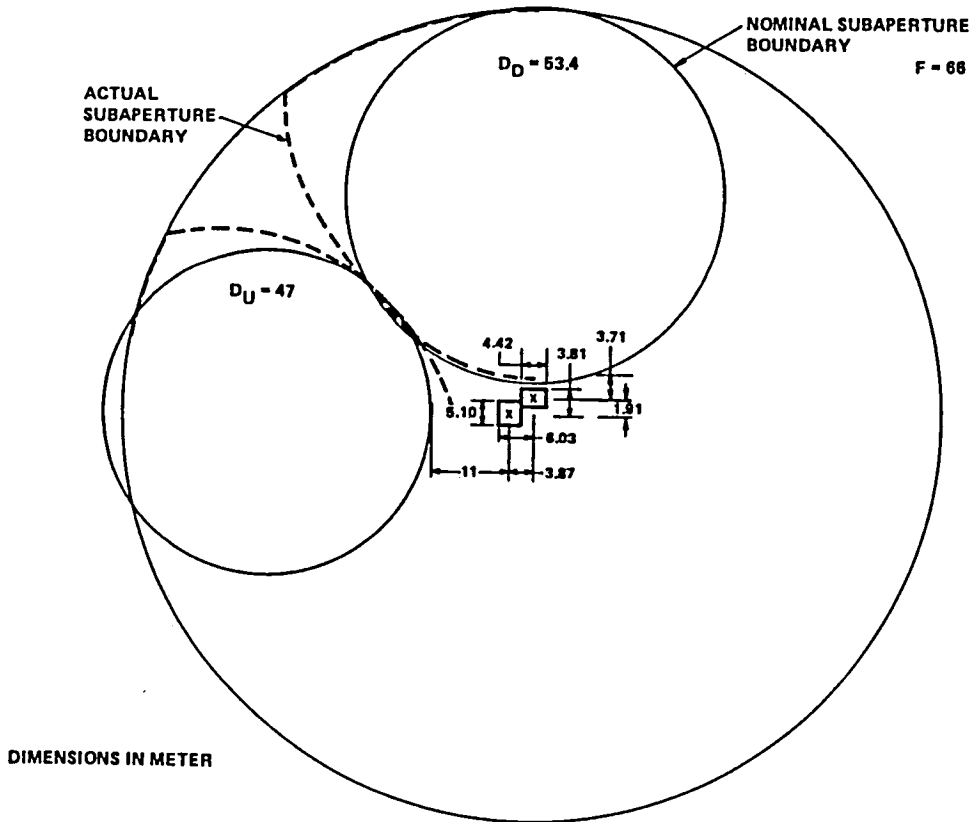


Figure 4.1.- Front view of the quad antenna aperture (E/W side solar array implementation).

earlier. The plan shows that for UHF the nominal downlink aperture is 53.4 m, while the nominal uplink aperture is 47 m. The larger downlink aperture provides about 3 dB more gain than the uplink aperture, and thus minimizes the RF transmit power requirement for a given EIRP. The uplink antenna diameter is still compatible with the beam isolation requirement. At the same time the geometry allows the use of solar arrays on the east and west side of the feed system.

Figure 4.2 shows the reflector and feed profiles of the UHF downlink antenna.

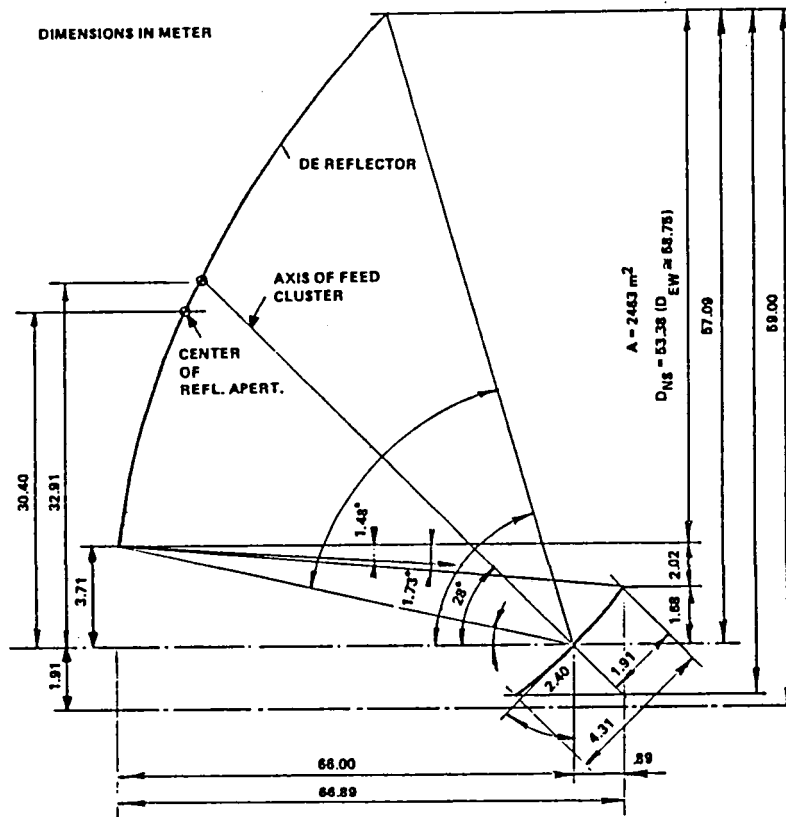


Figure 4.2.- Optics geometry in the NS plane, N side of the UHF downlink antenna (E/W side solar array implementation).

Figure 4.3 shows the reflector and feed profiles of the UHF uplink antenna.

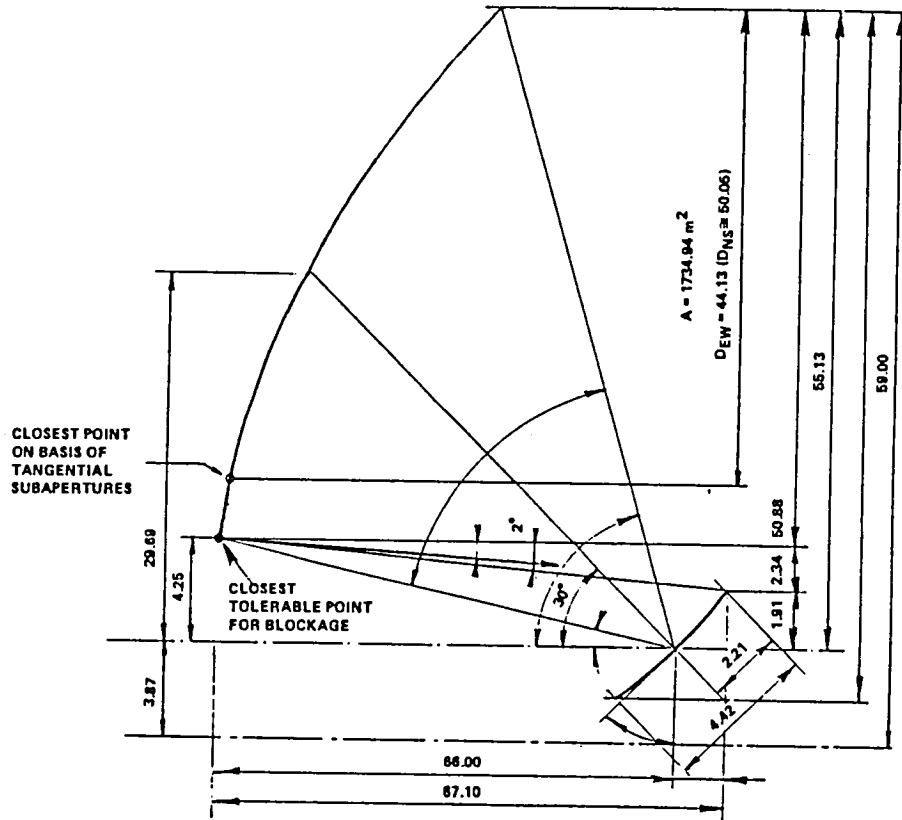


Figure 4.3.- Optics geometry in the EW plan, E side of the UHF uplink antenna (E/W side solar array implementation).

There are a number of interesting features in the geometry exhibited on figures 4.1, 4.2, and 4.3. The reflectors associated to the sub-apertures are offset sections of revolutionary paraboloids with a common focal length of $F = 66$ m. The axes of these paraboloids do not converge at the same focal point. The axes, however, are kept parallel to each other. The axes form a rectangle with diagonals of 3.82 m and 7.74 m. Thus, while the individual reflectors are revolutionary surfaces, the resultant reflecting surface is not. The resultant reflecting surface still has two symmetry planes, the NS

and EW plane of the structure. The downlink and uplink reflectors have an F/D of 1.235 and 1.404, respectively. These F/D values were selected somewhat conservatively in order to meet the specified beam isolation values. A slight reduction may be feasible in a second iteration. The focal distance of the reflectors do not have to be equal. In a more refined design these may be selected with slight differences to relocate some scatter side-lobes which are associated by unwanted coupling between a downlink feed with an uplink reflector or uplink feed with a downlink reflector.

The inner points of the reflectors are determined by the so-called "last intercepted ray." This last intercepted ray is defined on a geometrical optical basis. It originates from a boundary located feed and after being reflected by the edgepoint of the reflector it misses the feed array boundary by one secondary pattern beamwidth. No reflector should be extended beyond this point in order to avoid the scatter from the feed array.

Another point can be defined on a given reflector profile for the boundary of the reflector, on the basis that the four sub-apertures are tangential to each other. For the presently selected unequal downlink and uplink sub-apertures, the boundary of the sub-apertures projects an elliptical shape to the common overall aperture. The inner points of these projections are generally further away from the axes of the paraboloid than the points defined by the last intercepted rays. Thus, the region between the two boundaries can be filled with reflecting surface.

Similarly the reflector surfaces can be extended beyond the circular (or elliptical) boundaries in the region between the sub-apertures. Referring to figure 4.1, the limit of these extensions is a compromise between increasing antenna gain and increasing unwanted coupling between a feed and the wrong sub-aperture. While in practice the sub-aperture boundary can be along the

dotted line shown on figure 4.1, the present RF calculations will be done for the approximate elliptical boundaries with the exhibited average sub-aperture diameters.

Figure 4.4 illustrates the feed array geometry necessary for the optics shown on figures 4.1 to 4.3. The sidelobe controlling "half width" radiating elements along the east-west dividing lines of the feed array, and along the north and south border are not shown on this figure. After, when the four feeds are deployed in their operational positions their projected envelope to

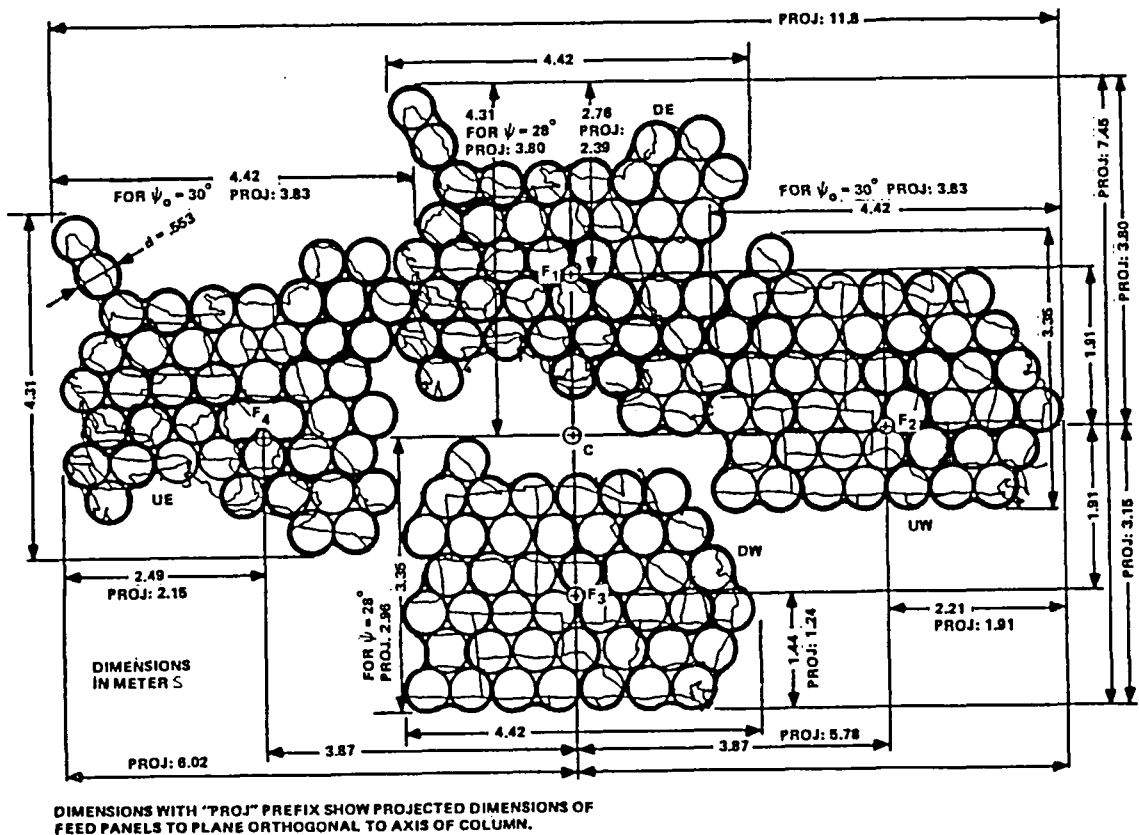


Figure 4.4.- Geometry of the feed layout.

the aperture plane is within an 11.8 m x 6.95 m rectangle. The F_1 , F_2 , F_3 , and F_4 points indicate the location of the focal points of the sub-apertures of the quad antenna.

Figure 4.5 shows one possible physical implementation of the feed defined by the geometry on figure 4.4. Each of the feed arrays are divided into two or three feed panels which can be folded for the shuttle stowed configuration. During launch the plane of these panels is parallel to the axis of the shuttle. In the operational position the panels are unfolded and tilted to 28° or 30° relative to the aperture plane of the overall quad antenna. The

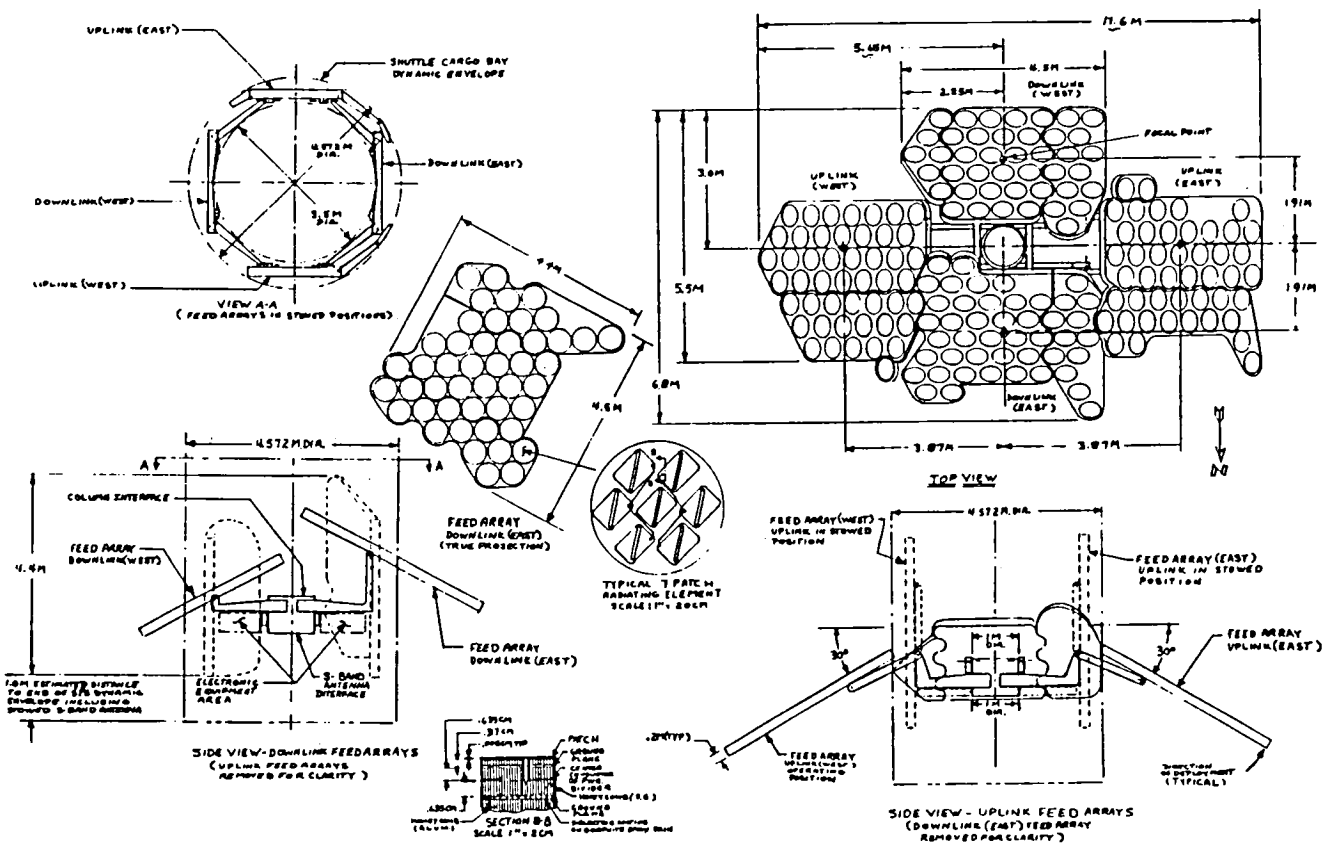


Figure 4.5.- UHF feed configuration.

feed system is composed of printed radiating elements (sub-arrays), printed power dividers and monolithical transmit and receive RF electronics. These are all integrated inside the panels. The beam forming network (BFN) makes use of flexible coaxial cables for the power connections in the system. This permits the panels to unfold during deployment.

The geometry of the antenna defined in the above discussed figures must be maintained with a high degree of accuracy in order that the necessary beam isolation is realized and the beam pointing is acceptable.

Table 4.1 summarizes the most important tolerance requirements of the antenna.

TABLE 4.1.- SUMMARY OF THE MOST IMPORTANT ANTENNA TOLERANCES

Characteristics	Value
Reflector surface accuracy, rms	0.42 cm
Pointing accuracy of overall structure, peak	
Variation within 1 min	0.07°
Variation within 5 min	0.10°
Absolute pointing inaccuracy relative to nominal, long term	0.14°
Lateral position of feed panel (in plane perpendicular to axis of antenna)	±6.6 cm
Axial position of feed panel	±10 cm
Tilt of feed panel relative to nominal	±0.3°
Flatness of feed panel	±0.5° cm
Axis of sub-aperture relative to common axis of structure	±0.02°

For the geometry discussed previously solar arrays mounted in the vicinity of the feeds must be on the east and/or west side of the feed arrays. It is easy to modify this configuration to allow north and south side mounted solar arrays. For such an arrangement the position of the uplink and

downlink systems are interchanged. Due to the frequency band differences and the contour shape of the feed arrays the net effect of such an interchange is some reduction in the diameter of the downlink sub-aperture. Figures 4.6 to 4.8 illustrate the applicable geometry.

Figure 4.6 shows a quad antenna geometry in which the uplink sub-apertures are in the N-S plane and the downlink sub-apertures in the E-W plane. This configuration reduces the total available aperture area for the downlink antennas, but provides an alternative in which the solar arrays can be on the north and south side of the feed array, where only a single-axis drive is required.

Figure 4.7 shows the reflector and feed profile in the N-S plane for the case where the solar array is on the north and south side of the feed array.

Figure 4.8 displays the feed geometries for the N-S plane solar array implementation. The layouts include the allowance for half-width radiating element extensions of the arrays for sidelobe control as previously discussed.

The two alternative geometries described above offer a choice between the best possible utilization of the overall aperture or the more convenient solar array arrangement.

The detailed structural layout was developed for the east-west mounted solar array, but a final configuration may use the second alternative. Consequently, the RF performance calculations have been developed for both cases. The calculations indicate that, from an RF point of view, the second alternative is less favorable, but the performance objectives can still be met. They also show that the most critical performance characteristic, the 25 dB beam isolation, can be met with a slightly smaller F/D ratio than the one selected. This in turn may allow some reduction in the length of the column and the associated feed array size.

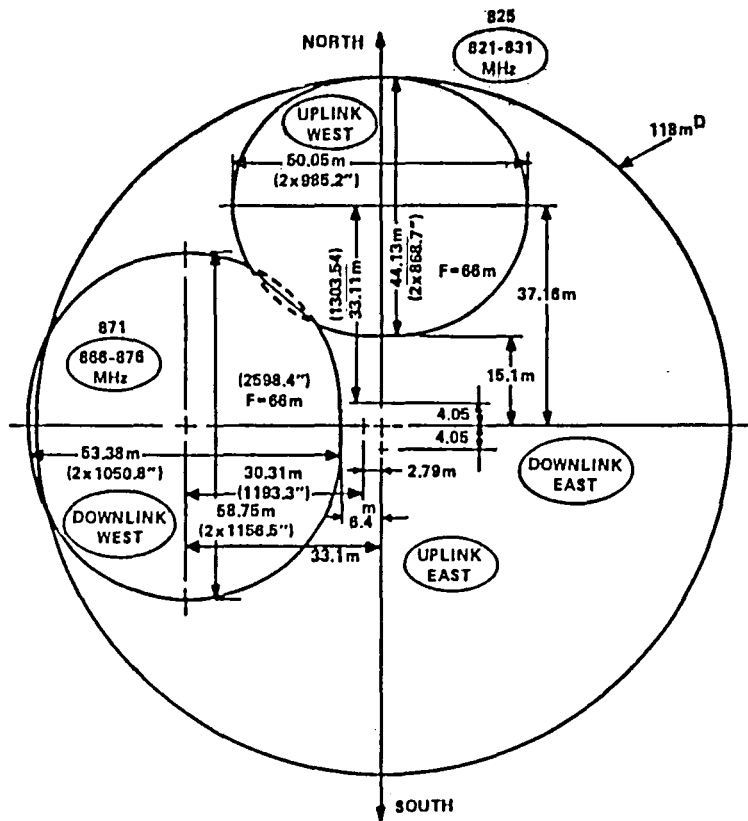


Figure 4.6.- Front view of the quad antenna N/S side solar array implementation.

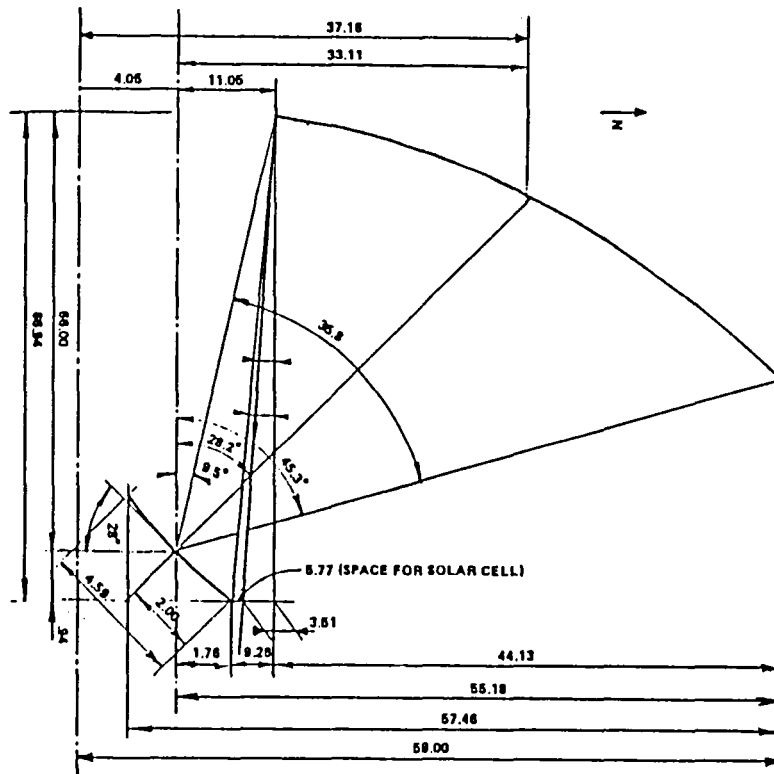


Figure 4.7.- Downlink optics geometry in NS plane for N/S side solar array implementation.

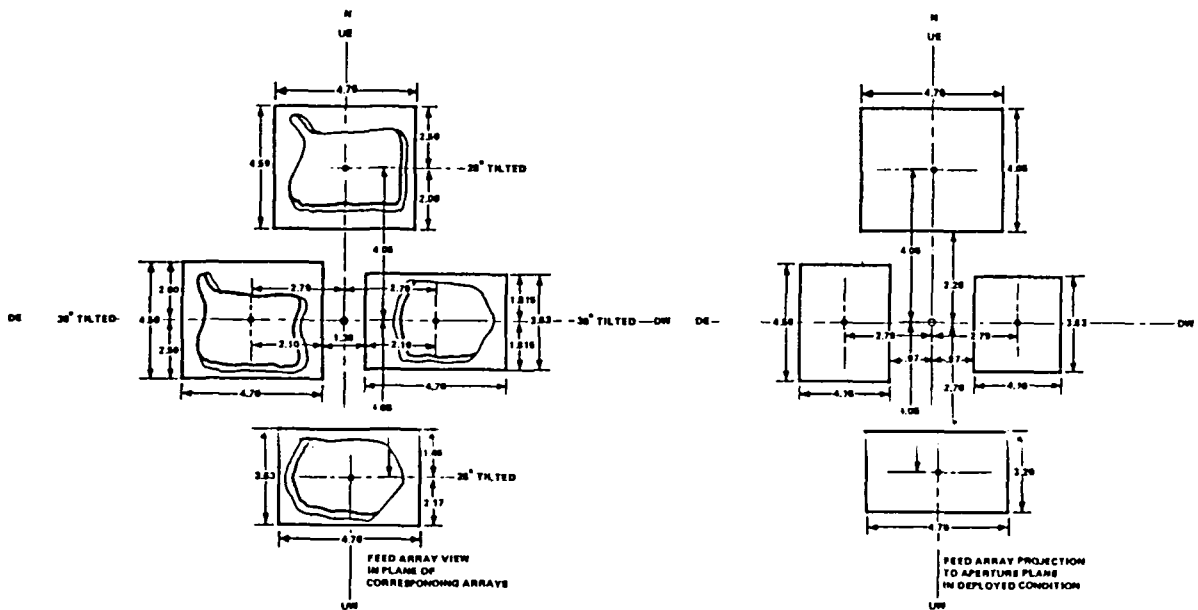


Figure 4.8.- Actual and projected boundaries of the feed panels for N/S side implemented solar arrays.

5. RADIATION CHARACTERISTICS FOR VARIOUS FEED IMPLEMENTATIONS

In the following discussion the radiation characteristics (gain contour) of the quad antenna will be presented for the various geometries and feed implementations. The results are obtained by computer simulation based on wave optics and appropriate approximation of the excitation of the radiating element.

The first series of calculations are for the downlink frequency band using the E-W mounted solar array geometry. The second series are for the uplink frequency band using the N-S mounted solar array geometry. This latter case represents the worst situation for gain and beam isolation. The corresponding two cases of interest (uplink, E-W mounted solar array and downlink, N-S mounted solar array) can be easily obtained by extrapolation. It is assumed that the radiating element will be realized as a printed array of up to $1-1/2\lambda$ diameter. For such small element size its radiation pattern can be

approximated by a $TE_{1,1}$ mode excited, open ended, circular waveguide without any major effect on the resultant secondary gain contours. Thus, for the sake of computational convenience most calculations are based on the pattern of a radiating source excited in the $TE_{1,1}$ mode.

Figure 5.1 illustrates the basic downlink radiation characteristics of a singlet beam of the quad antenna, realized by a single radiating element of approximately $1-1/2\lambda$ in diameter and excited by the $TE_{1,1}$ mode.

The diameter of this radiating element is selected in such manner that it allows the necessary $\alpha = 0.423^\circ$ cell size of the chosen beam topology. It can be seen, that for this radiating element size, providing about 5 dB taper at the edge of the sub-aperture, the level of the first sidelobe is only about 20 dB down for the on axis beam. For the selected beam topology the nearest cell using the same frequency and polarization is in the vicinity of the second sidelobe, which is 26 dB down. At the corner of the hexagonal cell contour the contour gain is ~ 6 dB down relative to the maximum. This configuration, then, gives about 20 dB beam isolation between two adjacent beams.

Figure 5.2 shows the beam in the maximum scanned position. In this case, the center of the beam is at Boston, and the sidelobe level in the nearest cell where interference could be a problem (marked by dotted line) is -24 dB.

For this case the beam isolation on the boundary of the 0.423° circular cell is 20 dB, and on the boundary of the hexagonal cell 18.5 dB. It must be emphasized that these isolation values are applicable for a single interfering adjacent beam. When all interfering power is added, approximately 1.5 dB more deterioration is experienced.

Configuration		DOWNLINK ANT
Geometry	D, in	2323 X 2087
	F/D	F = 2598 in
	Q, in	268
	d, in	21
	α , deg	0.423
n	1	
Beam		FOCUSED
Polarization	MAIN	CIRCULAR
Longitude, deg.		110 W
Antenna Axis	EW	
Pointing, Deg.	NS	
	EW Bias	
Frequency, GHz		0.856
Max. Gain, db		52.0

Figure 5.1.- Singlet gain contour for the unscanned singlet beam generated by a TE_{11} mode excited circular wave guide feed.

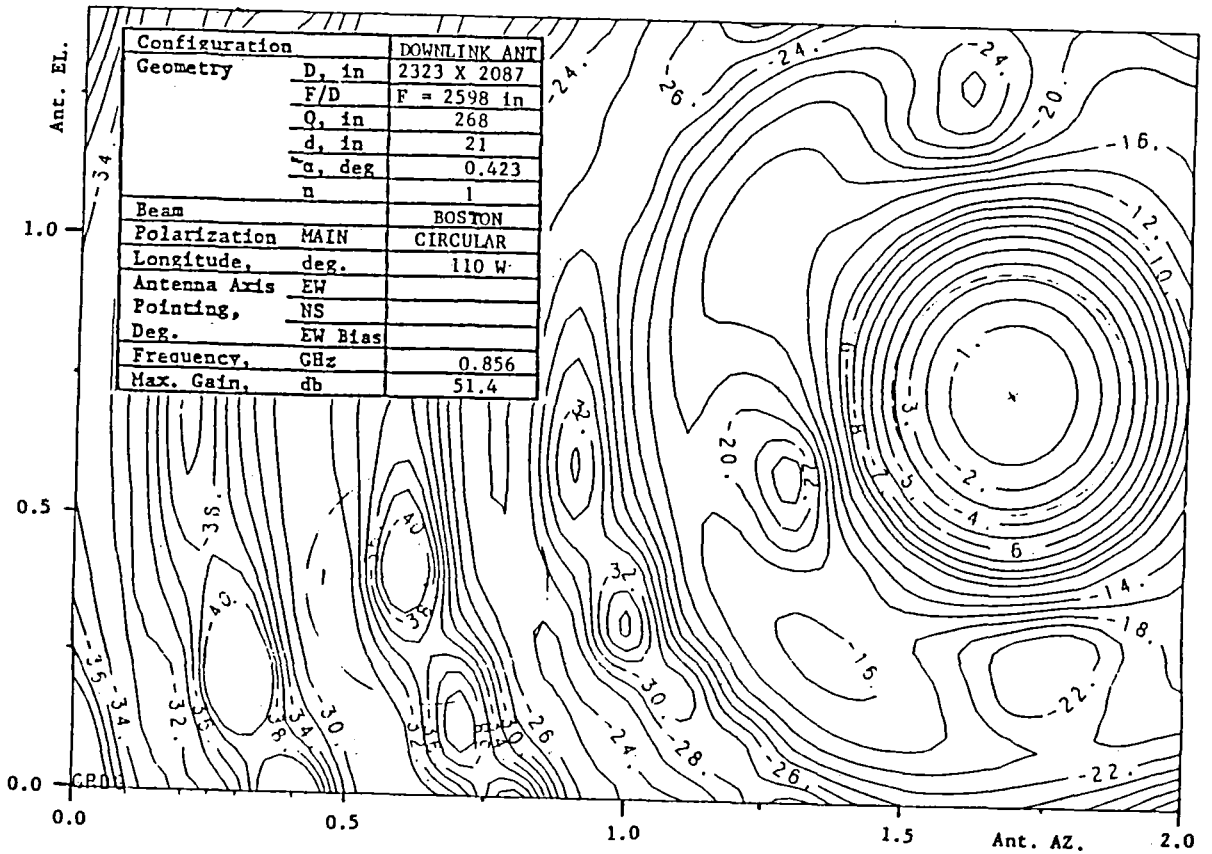
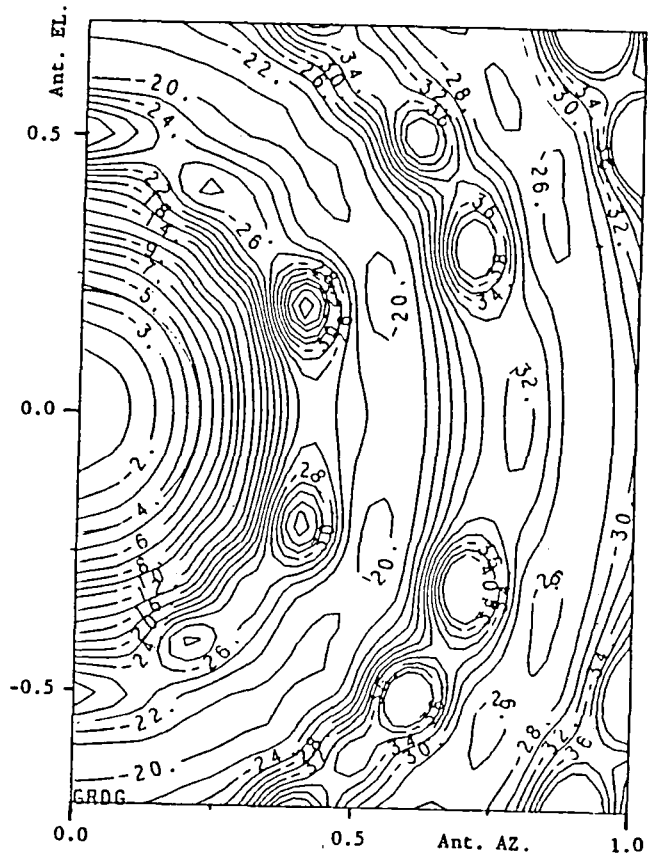


Figure 5.2.- Singlet beam contour in maximally scanned position.

It can be concluded from the above that for the selected F/D and scan angle of $\theta_M = 4.3\alpha$ a maximum beam isolation of approximately 17 dB is feasible with a single element feed. Even with infinite F/D , or no scan, only 18.5 dB beam isolation is achievable.

The peak gain of the antenna is 52 dB for the on axis beam, without any circuit loss, inaccuracy effects, or blockage. This represents $\eta = -2$ dB (63 percent) antenna efficiency. For the maximally scanned beam the peak gain drops to 51.4 dB but the contour gain actually increases relative to the unscanned beam. (On the circular boundary it is 47 dB for the on axis and 47.4 dB for the scanned beam.)

Figure 5.3 indicates the gain contours if the radiating element is replaced by a seven-element sub-array instead of the TE_{11} waveguide mode

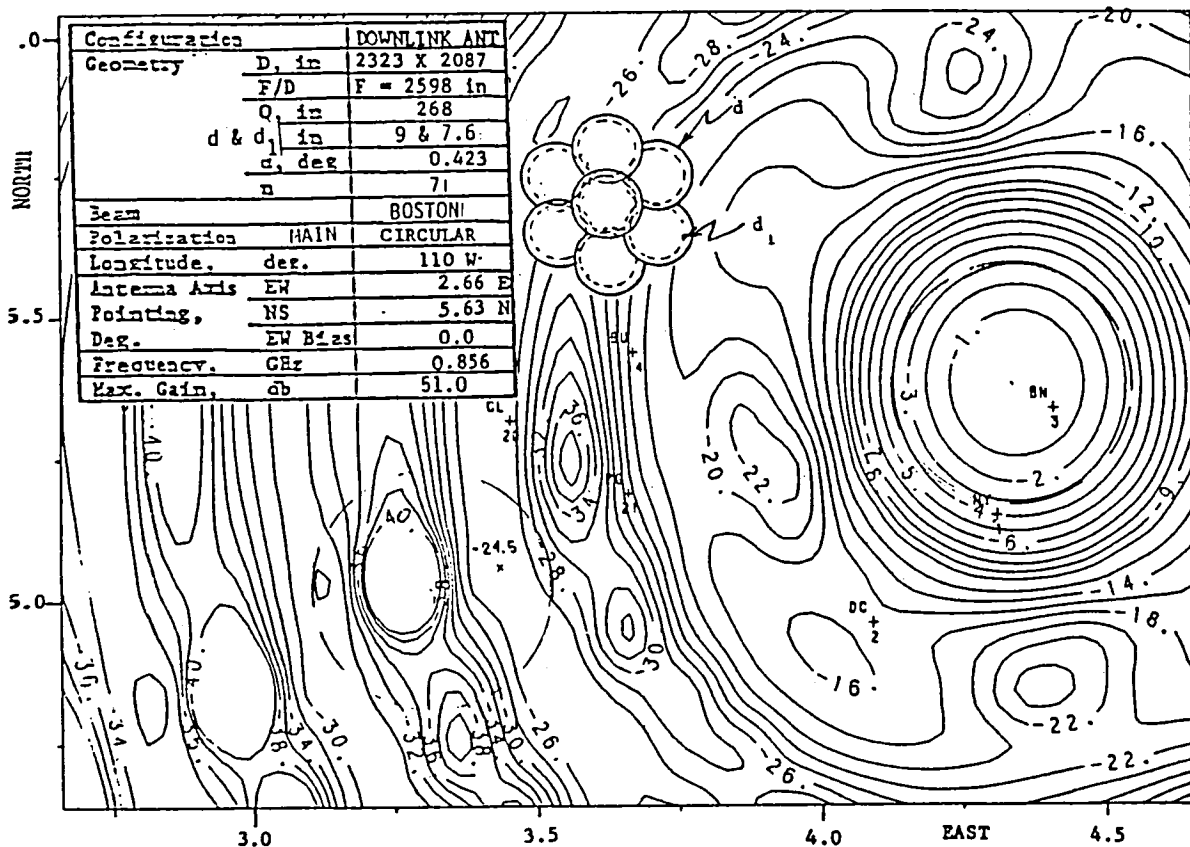


Figure 5.3.- Maximally scanned singlet beam contour generated by a seven-element sub-array.

field distribution used for figure 5.2. It can be seen that the gain contours are nearly identical to the previously calculated ones and the adjacent beam isolation is still only 20.5 dB on the circular contour.

It can be concluded from these calculations that a single $1-1/2\lambda$ diameter radiating element, whether it is a single radiator or a sub-array is not capable of producing beams with 25 dB isolation with the selected optics geometry and beam topology.

A comparison between figures 5.2 and 5.3 also indicates that the relatively large change of field distribution within the 1.5λ diameter overall radiating element aperture has only a small effect on the shape of the secondary gain contours.

Figure 5.4 indicates downlink gain contours of a possible feed configuration which is approximately compatible with the 25 dB beam isolation requirement, selected geometry, and beam topology plan. The configuration uses a so-called "doublet" feed, consisting of two radiating elements (one main and one auxiliary) with 1.0 and 0.1 unit power excitation. The sidelobe level of the "Boston" beam is -32 dB in the nearest interfered cell. Since three additional nearby interferers might produce sidelobes in this cell it is possible that the resultant could be -26 dB. As the main beam at cell contour is -3 dB for this condition the resultant C/I ratio may be 23 dB. With optimization of the excitation levels of the elements in the doublet it can be expected that the maximum sidelobe of the interfering signals in the interfered cell are not occurring at the same angle. For this case the C/I can be further improved.

The beam topology plan shown in figure 3.1 indicates that any beam can create major interference at least in four nearby cells, thus the sidelobe

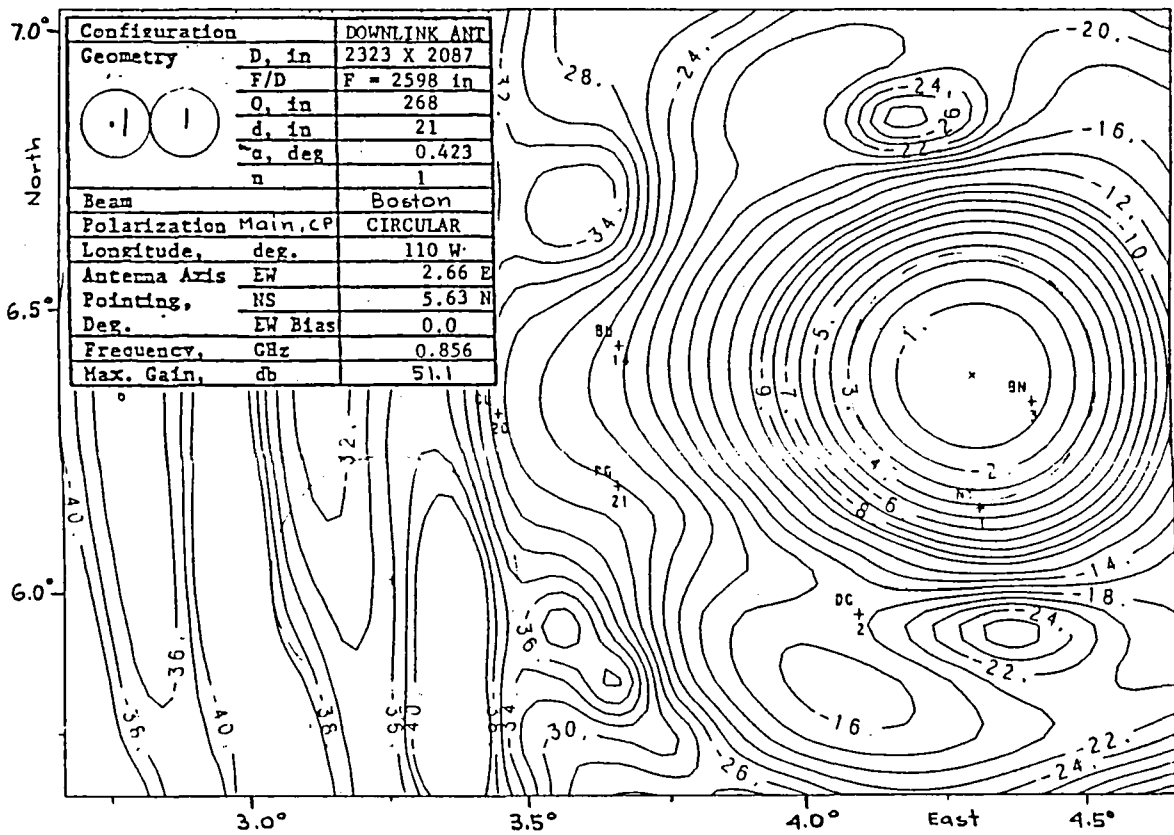


Figure 5.4.- Sidelobe control achievable by a doublet feed.

control principle shown in figure 5.4 generally needs four auxiliary radiating elements, yielding a five-element feed cluster for the generation of each pencil beam.

A further improvement of sidelobe level can be obtained if the auxiliary elements are increased to 6. In this case the resulting feed is hexagonally symmetrical and consists of seven elements. The gain contours are shown in figure 5.5 for 0 dB center and -10 dB outer element excitation. The peak gain is reduced from 51.4 dB (with single element feed) to 50 dB but the edge gain is still 48 dB and the sidelobe level is -38 dB down in the interfered cell. This provides 36 dB adjacent beam isolation. The resultant C/I of the complete system is still nearly 36 dB because the peaks of the interfering sidelobes from the different adjacent beams occur at different angles.

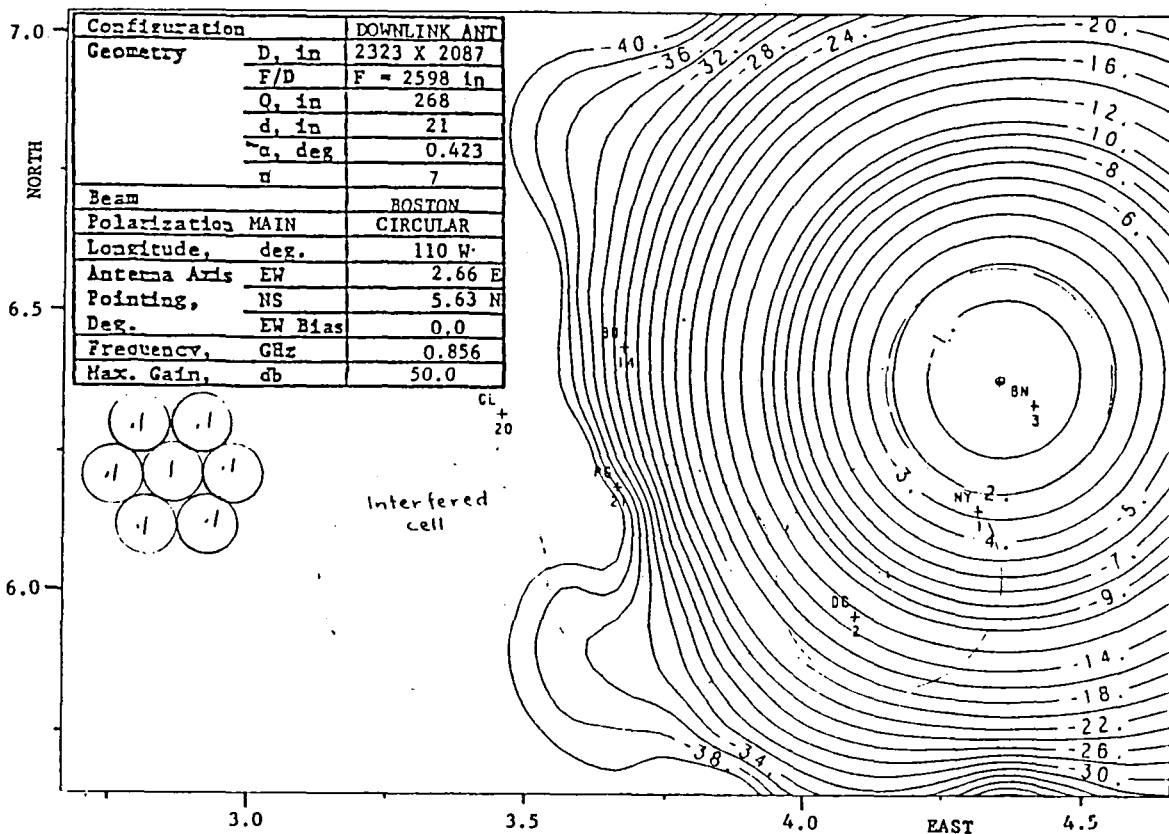


Figure 5.5.- Sidelobe control with a seven-element feed.

The contour gain with this feed is approximately 47 dB without circuit losses and 46.8 dB with the assumed circuit losses. This leaves a 1 dB margin relative to the value stipulated in table 2.4.

It must be recognized that the seven-element feed cluster, whose contours are shown in figure 5.5, represents not only a large improvement in the isolation characteristics of the antenna but also a significant increase in complexity. Instead of connecting a single transmitter to a single radiating source, a transmitter now has to be connected to seven sources via a power divider, beam forming network (BFN). Additionally, due to the contiguous coverage requirement, the feeds of adjacent component beams must share some of the radiating elements, and the adjacent feeds must overlap. Furthermore, for the selected beam topology plan, some of the adjacent component beams are

oppositely polarized, which means that all the radiating elements must have dual polarization capability.

The next discussion of results concerns the N-S plane solar array related geometry.

Figure 5.6 shows the uplink gain contours for the maximally scanned beam when the solar arrays are installed in the north-south plane. For the singlet the level is -24 dB in the interfered cell.

The applicable sidelobe level is the same as with the corresponding down-link case shown in figure 5.6. However, the sidelobe peak now is in the middle of the interfered cell instead of at the edge, and tends to increase if there is more than one interfering signal.

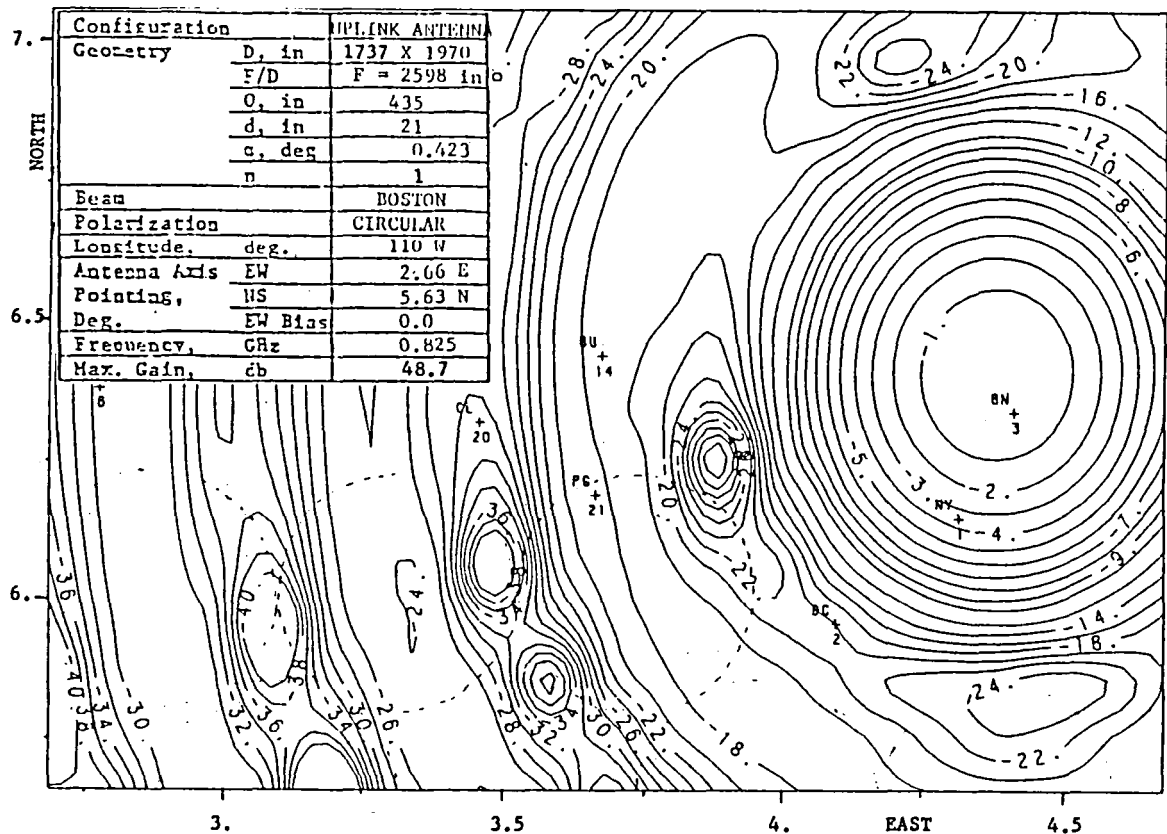


Figure 5.6.- Singlet gain contour for the maximally scanned beam, UHF uplink.

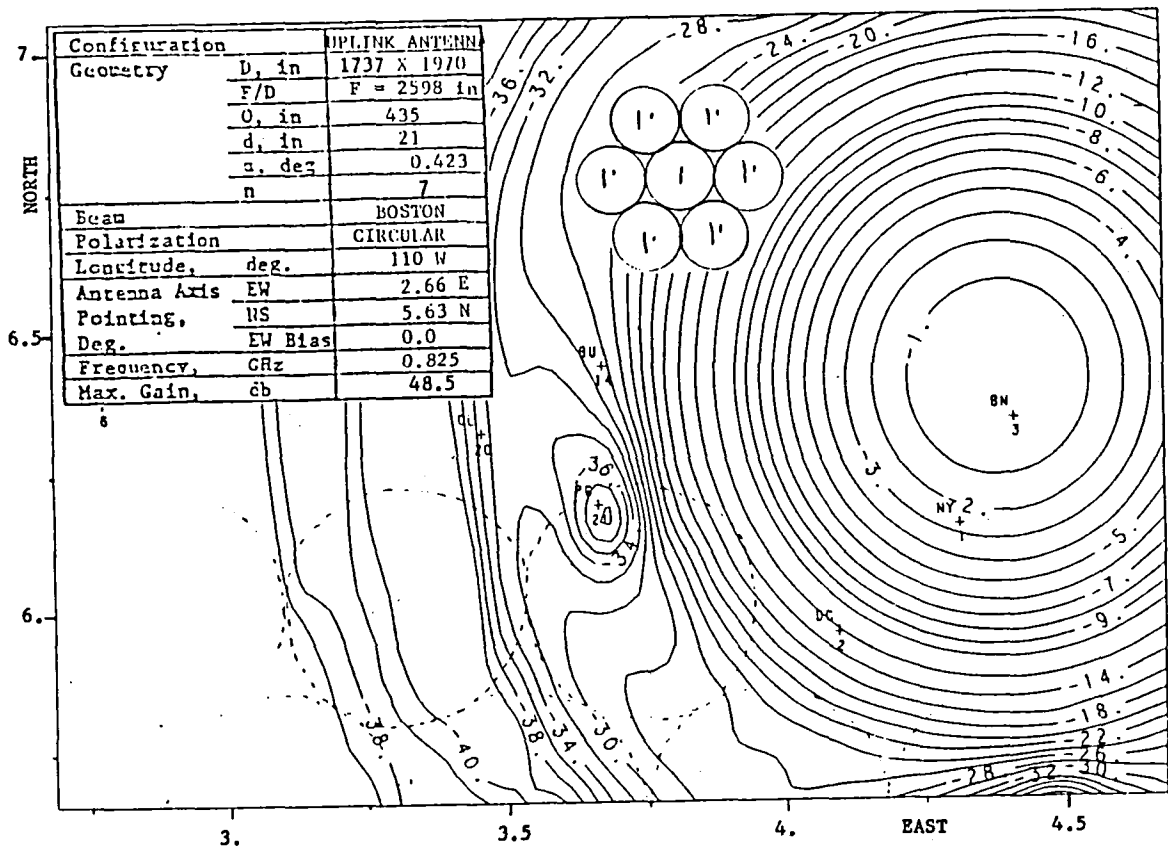


Figure 5.7.- Seven-element feed cluster gain contour for the maximally scanned beam, UHF uplink.

Figure 5.7 shows that for the seven-element cluster feed the sidelobe level is -32 dB. It can be seen that the combined effects of the 90° rotation of the quad antenna, the smaller sub-aperture diameter, and the lower frequency cause a 6 dB deterioration relative to the corresponding sidelobe level of the downlink antenna (fig. 5.5). However, the resultant sidelobe level from four nearby interfering sources is still -30 dB yielding C/I = 28 dB, which meets the specification.

The uplink contour gain is approximately 45.5 dB, without circuit losses, for this configuration; this is about 1.5 dB lower than that of the downlink antenna.

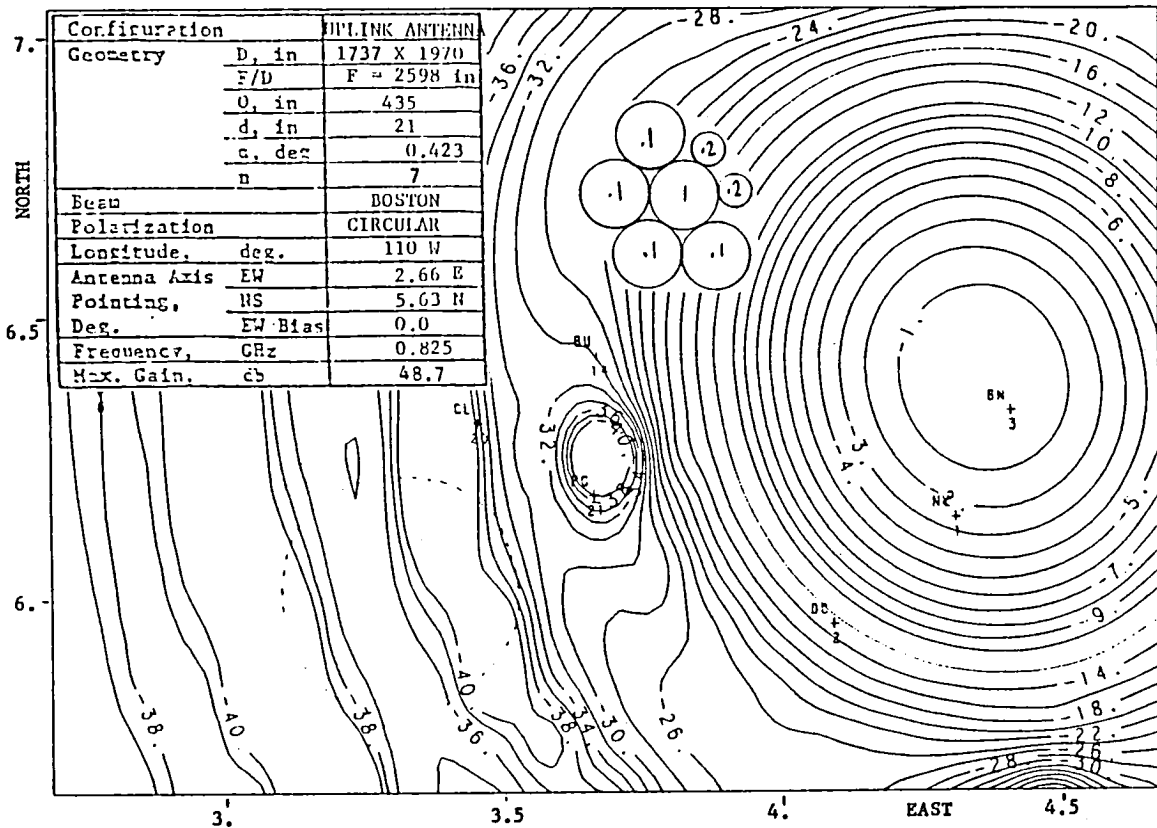


Figure 5.8.- Gain contours for nonstandard seven-element clusters configured for coverage boundary application.

Figure 5.8 exhibits the effect of the diameter reduction of two of the six auxiliary elements in the seven-element cluster. Such elements are desirable for boundary located feeds in order to achieve the necessary side-lobe control outside the coverage area without significant increase in overall-feed panel size. The reduced elements have half the standard $1-1/2\lambda$ diameter but this is compensated for by higher power excitation. The calculated gain contour differs very little from the gain contour of the standard element (fig. 5.7) but still yields approximately 28 dB resultant C/I.

Thus, it can be concluded that it is feasible to use half-width radiating elements for sidelobe control purposes in the boundary region of the overall coverage area. This minimizes the penalty associated with the division of the

overall feed array for an east and west section, as needed for the implementation of the quad antenna.

With the selected beam topology plan, implementation of the seven-element feed clusters requires that each radiating element in the feed (in general) has a dual polarization capability. The reason for this is that they must act simultaneously as main and auxiliary radiator (for different coverage cells) and these could be of opposite polarization. If a maximum of four auxiliary radiating elements are needed for any beam, it is possible to select their corresponding radiating elements in the overall feed array so that only elements of one polarization are necessary.

Figure 5.9 shows such a configuration. The center interfered cell receives sidelobe power from adjacent identical frequency and polarization

Configuration		AMPLINK ANTENNA
Geometry	D, in	1737 X 1970
	F/D	F = 2598 in
	Q, in	435
	d, in	21
	a, deg	0.423
	n	8
Beam		BOSTON
Polarization		CIRCULAR
Longitude, deg.		110 W
Antenna Axis	EW	2.66 E
Pointing,	US	5.63 N
Deg.	EW Bias	0.0
Frequency,	GHz	0.825
Max. Gain,	db	48.7

4 Auxiliary horns are used to reduce central interference level from -16 dB to -26 dB.

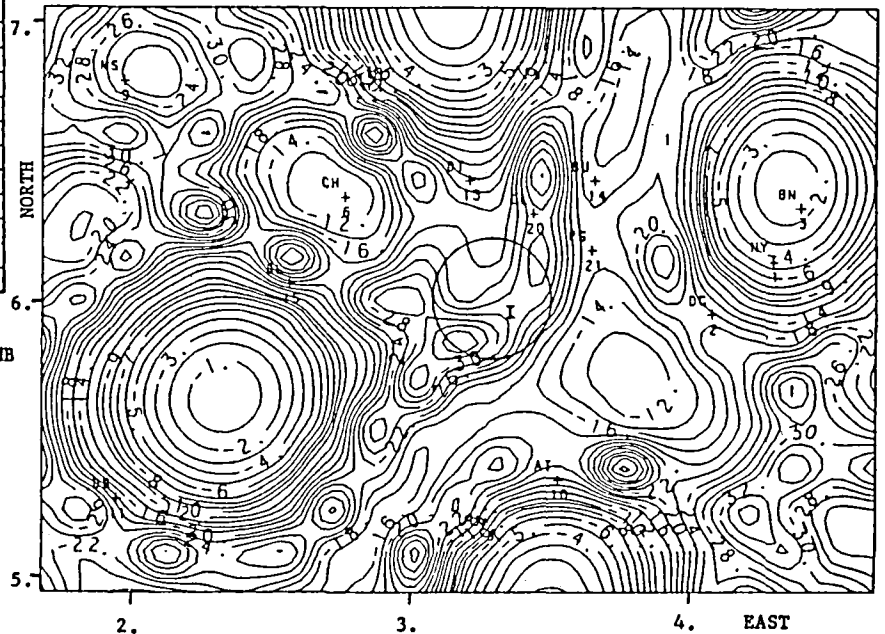
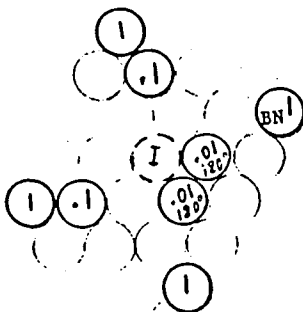


Figure 5.9.- Use of five-element feed cluster requiring only single polarized radiating element.

beams. Each of these main beams carry one unit of power. The selected auxiliary horns carry either 10 dB or 20 dB lower power level and their location is chosen so that they are compatible with singular polarized radiating elements. In the center, interfered cell, the sidelobe level is -16 dB without the auxiliary horns. This improves to -26 dB with the selected excitation. The resultant C/I = 24 dB is somewhat marginal, but it must be noted that no great effort was devoted to optimize the excitations. The values of the achieved C/I indicates the feasibility of the concept.

In a practical configuration each interfering beam could produce objectionable sidelobe power in four critical cells. Thus each feed cluster must carry four auxiliary elements. The excitation of these four elements relative to the center (main) element has to be synthesized individually for each beam. This gives rise to some complexity for a large multibeam system, but in principle represents no specific difficulties. The synthesis can be set to produce secondary patterns with nulls in the middle of each adjacent interfered cell, or a minimum throughout the entire interfered cell. The employment of this concept is quite significant, because it simplifies the complexity of the beam forming network in a 5/7 ratio and allows the use of singular polarized radiating elements.

During the study program RF calculations were carried out for the selected baseline quad antenna configuration in which the four apertures were divided between uplink-downlink and east-west coverage functions. (See case F in table 2.5.) In these calculations, one major aim was to simplify the BFN at the expense of some reduction in the maximum achievable beam isolation.

Another impressive simplification of BFN may be achievable by using the case E configuration of table 2.5. The prerequisite for this configuration is a single polarized radiating element, which can cover simultaneously the

uplink and downlink frequency bands. In this case the radiating element diameter can be increased to $d = 2.74\lambda$ which assures a sidelobe level approximately compatible with the isolation requirement. Under these conditions no feed overlap occurs, but one diplexer must be provided for each feed cluster. Since the radiating element (sub-arrays) are now larger, the loss in the feed arrays itself is larger and it is added to the diplexer loss. Furthermore, the Θ_M/α value of the system is doubled; thus the contour gain decreases with scan angle instead of increasing, as it does in the baseline configuration.

The combined effects of these factors are not clear, but because the approach has some attractive features, it appears to be worth future investigation.

In the quad aperture configuration, ideally each sub-aperture is illuminated only by its corresponding feed cluster. In practice this situation cannot be achieved because the size of each feed cluster forming a beam is finite, thus the beam radiates some of its power outside the solid angle about the axis through the center of the cluster toward the edge of the sub-aperture. Some of this power misses the overall antenna system and becomes a spillover radiation sidelobe, more than 110° away from the main lobe. As this radiation does not reach the Earth, it does not create an interference problem, but it does reduce system efficiency. Another part of this spillover radiation is captured by the other sub-apertures, which can refocus it into secondary beams. The largest of these beams are found in the left and right adjacent sub-apertures and they may be called "parasitic sidelobes."

Their location can be easily predicted on the basis of the location of the responsible feed cluster relative to the focal point of the adjacent sub-aperture. The amplitude of this sidelobe, compared to the main lobe, is

dependent on the aperture distribution, caused by the feed cluster in question, over the surface of the adjacent reflector segment. This requires a more involved calculation of the scattered field at relatively large angles from the axis of the adjacent sub-dish. For an actual mobile communication mission covering the U.S., most of the parasitic sidelobes fall outside the coverage area and into the Atlantic and Pacific Oceans. However, a few of them may fall into the southern part of Mexico or into the northern part of Canada, if these countries should employ a frequency plan independent of the U.S. This may generate a requirement to suppress these particular parasitic sidelobes to a level where they cause negligible interference. Due to the other limitations already in the system, the suppression of the parasitic sidelobe below about -24 dB does not make a significant contribution to overall interference reduction.

During this study, some limited investigations were completed to explore the ways to reduce the parasitic sidelobe problem. In principle, the following methods are available:

1. Increase the diameter and aperture taper within the critical feed clusters.
2. Use shroud plates to shield the adjacent sub-apertures from the unwanted radiation.
3. Eliminate those reflecting surfaces which are not part of the desired sub-dishes.
4. Reduce the diameters of the sub-apertures in order to create a gap between illuminated reflector segments.

The first method requires cluster diameters in the 1.5λ to 4.5λ range. If the basic sub-aperture in the feed array is 1.5λ in diameter, then a seven-element cluster of such sub-arrays allows relatively easily implementable

overlapping beams, which may be a requirement for the maximally scanned beams. It should be noted that practically all the geometrically objectionable parasitic sidelobes are associated with maximally scanned beams. Thus for such cases a 4.5λ cluster diameter is available.

In one specific configuration, the 1.5λ diameter sub-array must be implemented by four patches. For this case the total number of patches within the 4.5λ diameter resultant cluster is 28. Calculations indicate that this number is adequate to achieve at least a 28 dB parasitic sidelobe level with an appropriate aperture taper. The total number of patches probably can be reduced to 19 in order to get acceptable parasitic sidelobe suppression by this method. It must be pointed out that the layout of the grid within the 5.4λ diameter cluster plays an important role in the achievable sidelobe level, due to the grating lobe level associated to such a grid. Since the unwanted sub-apertures are in the left and right direction from the desired sub-aperture the minimum distance between the patch elements must be also in these directions.

The second method (shroud) offers a 3 dB to 6 dB suppression for a shroud size which is comparable with the area of the overall feed cluster. This method is electrically simple, because it does not involve additional complexity in the BFN. However, the method requires the deployment of mesh panels, which somewhat complicates the mechanical design.

The third method was not investigated in detail, but it seems to be attractive, because it introduces minimum system complication. At least 3 dB sidelobe suppression can be expected by this method.

The fourth method reduces the parasitic sidelobe in a well predictable manner and can again produce improvements up to 3 dB. However, even up to

this level the gain and resolution of the system deteriorates in an economically undesirable manner.

In summary, it appears that the parasitic sidelobe problem can be handled in a number of ways, and in a practical situation a combination of these methods could yield an acceptable solution.

6. FEED CONFIGURATION ALTERNATIVES

In order to concentrate most of the radiated power of the feed toward the sub-aperture for the selected F/D ratio, the diameter of the feed cluster must be at least 1.5λ . Additional aperture area is required for a better control of the distribution of the field in the aperture of the sub-dish for achieving the desired beam isolation. Such aperture size cannot be achieved with a single conventional patch radiating element. Consequently, several of these patches must be combined into a larger assembly, called a sub-array. Since the sub-array must have, as much as possible, axially symmetrical radiation, pattern patch combinations of 3, 4, 7, and 19 have the greatest interest. In the following discussion, examples for the four- and seven-element sub-array are presented.

The feeding of these patches can be divided into two categories: (a) the transmission lines are on the same substrate as the radiators, and can also radiate to some extent; and (b) the transmission lines are on a separate substrate.

Where the parasitic radiation cannot be tolerated, or the patch density is beyond four per 1.5λ diameter area, only the second method is usable. Shown below are examples for both layouts.

Figure 6.1 shows a four-element sub-array in which each element is an irregularly shaped printed patch, with a diagonal slot array. The geometry gives a relatively wide frequency band, and circular polarization within the

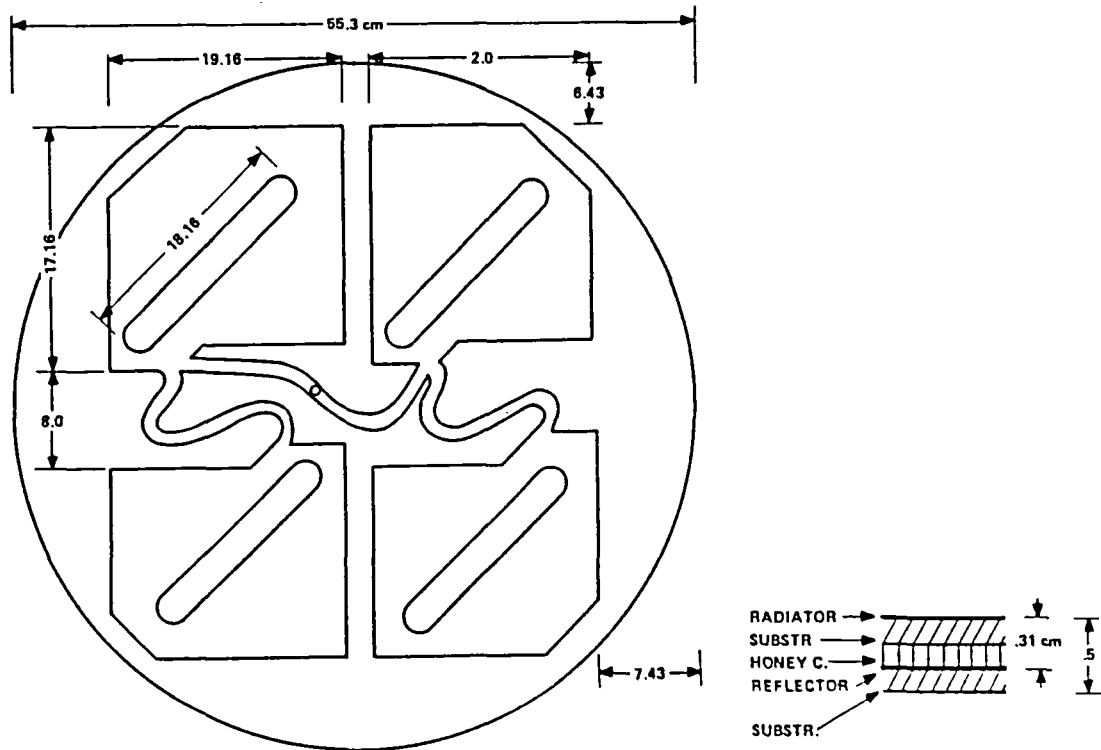


Figure 6.1.- Example for single polarized four-element sub-array.

required 36° full cone angle toward the reflecting surface of the sub-aperture. The combining network for the four patches is on the same substrate and the geometry is selected in such a way that their radiation is part of the overall circular polarization design.

Figure 6.2 shows a four-element sub-array capable of dual circular polarization. In this case the RCP power divider can be placed on the periphery of the four-element patch configuration, but the LCP power divider requires an additional printed circuit layer.

Both of these plans employ dual polarizations and a simple design (one or seven feeds per beam) for the satellite. The four frequency plan needs a somewhat larger F/D to achieve the beam isolation objective, but this plan was chosen on the basis that it utilizes a narrower bandwidth.

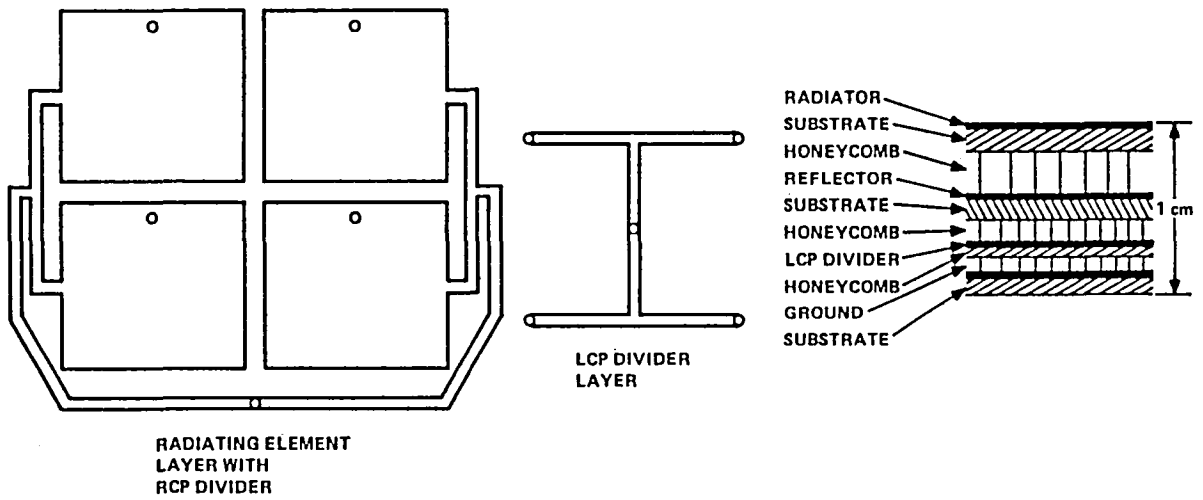


Figure 6.2.- Example for dual polarized, four-element sub-array radiating element implementation.

Figure 6.3 exhibits a seven-element sub-array. The shape of the patches is similar to those shown on figure 6.1, but due to the closeness of the

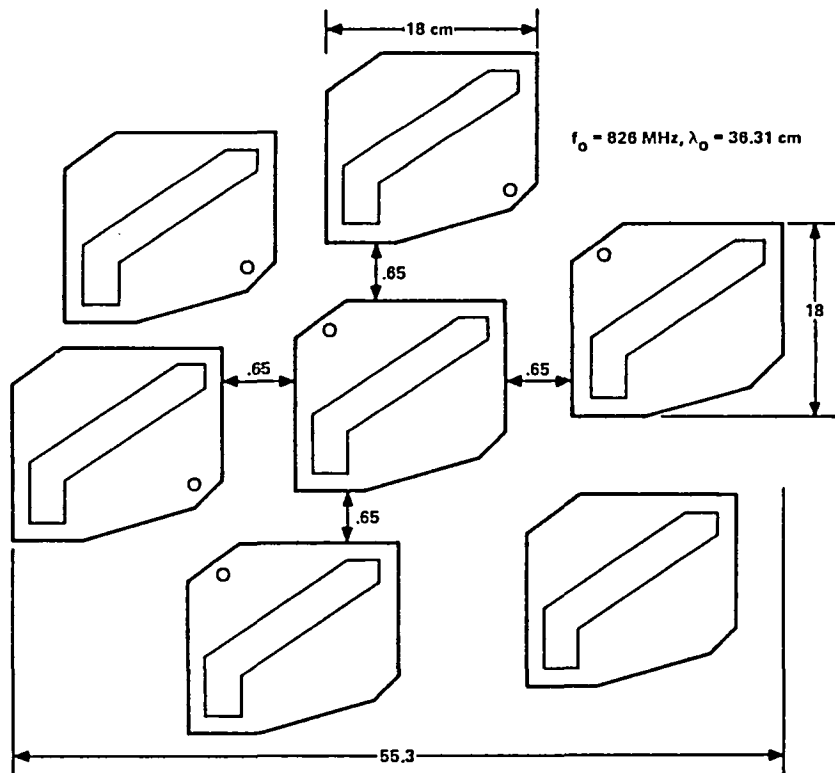


Figure 6.3.- Example for single polarized seven-element sub-array.

patches the power divider has to be placed on a separate printed circuit layer. (Two such extra layers are required if dual polarization is specified.)

It can be seen that the seven-element sub-array arrangement is much more complicated than for the four-element sub-array and it needs at least two printed circuit layers. However, it can be excited in a tapered manner (center element at 0 dB, outer elements at approximately -6 dB), which results in more symmetrical radiation pattern and smaller coupling between sub-arrays.

The beam forming network necessary to form multiple element (five to seven feed) clusters cannot be separated from the PA circuit layout design. The power for a given auxiliary radiating element must be taken off the signal leading to the main radiating element. The coupling can be done either in the input circuit, before the PA (fig. 6.4(a)) or in the output circuit after the PA (fig. 6.4(b)). In either case, the coupled signal must be further

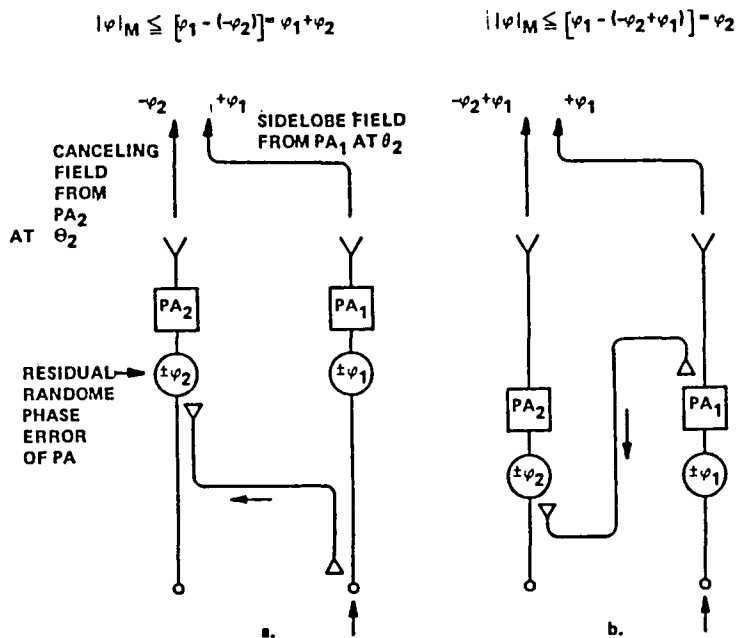


Figure 6.4.- Differential phase error introduced by random PA phase errors.

amplified in order that the total loss in the high power circuit is kept at a minimum. Since the sidelobe cancellation is based on the maintenance of the phases between the main and the auxiliary elements it is important that the effect of PA phase drifts is minimized. A common phase drift of the two PA's involved does not cause a change in the sidelobe cancellation. However, for the residual random (independent) phase errors associated with the individual PA's the scheme shown in figure 6.4(b) has smaller maximum phase error between cancelling radiated fields.

As to implementation, the two schemes differ very little in practice, thus only the figure 6.4(b) scheme will be discussed further.

Figure 6.5 shows the BFN-PA circuit implementation for dual-polarized radiating elements, using seven-element overall feed clusters. Note that two PA's (one at 0 dB, one at approximately -10 dB level) are needed for each radiating element.

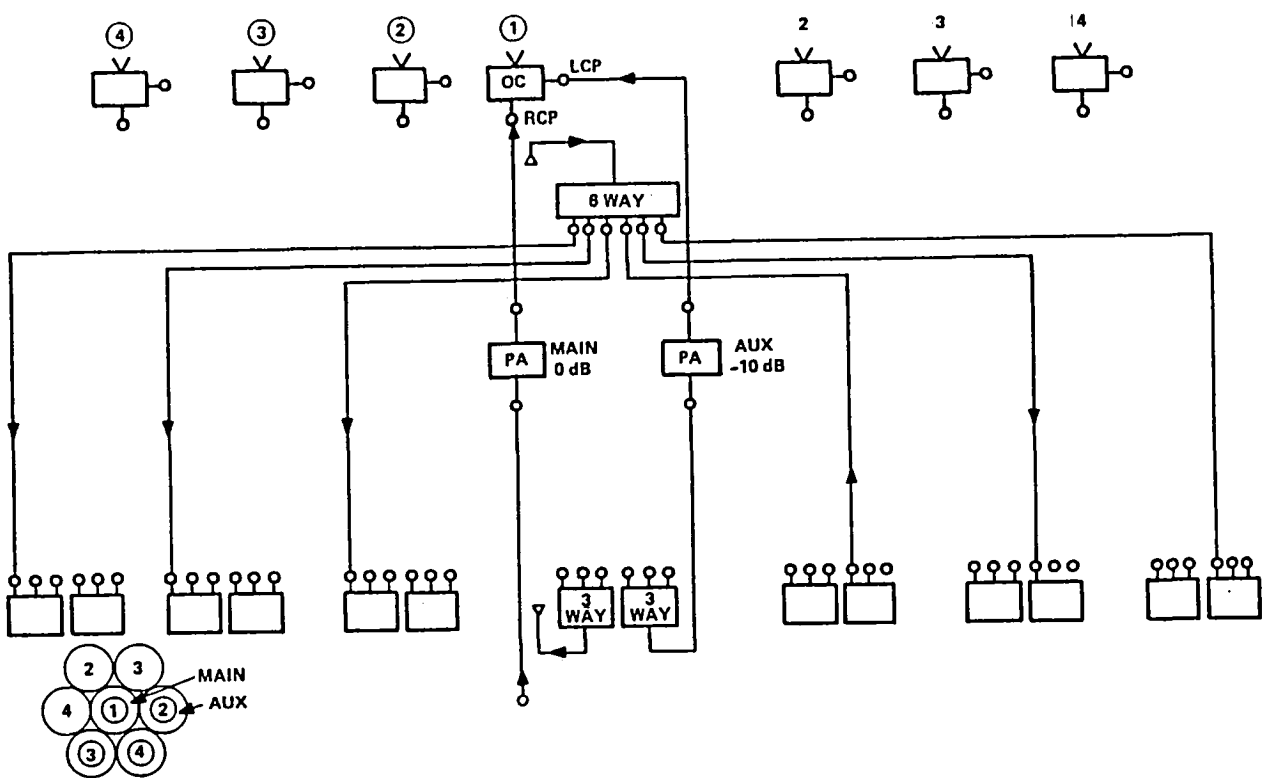


Figure 6.5.- BFN using dual polarized radiating elements.

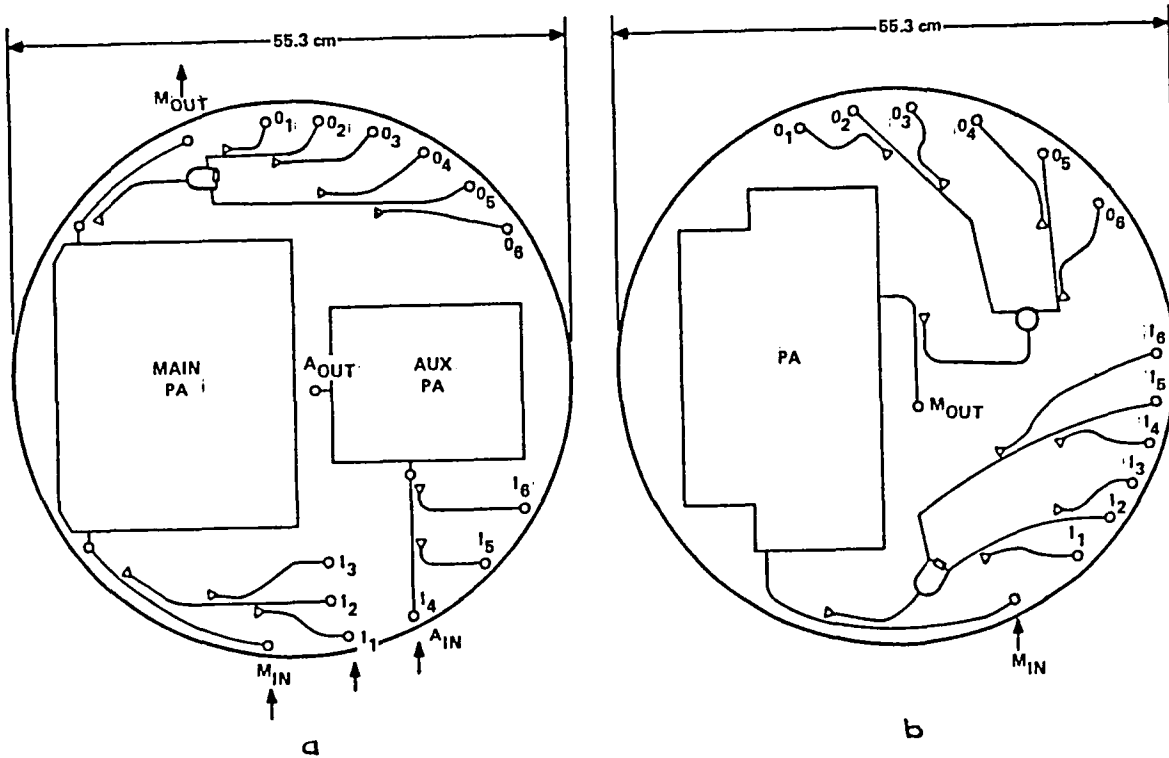


Figure 6.7.- Conceptual layout of BFN-PA circuit for dual and single polarized radiating element.

Figure 6.7(b) shows the PA configuration for the singular polarized case. Here more board space is available for the PA, and two identical 6-way dividers are provided, one at the input, one at the output of the PA. The terminal connections are similar to those described in figure 6.7(a).

7. S-BAND SUBSYSTEM

The purpose of the S-band subsystem is to provide the up and down communication links between the satellite and the base stations.

The S-band beam topology is determined by the S-band allocated bandwidth, minimum system complexity on the satellite and on the ground, and the simplest operational procedures.

System studies lead to an approximately 1:4 ratio between the number of S-band and UHF band beams. This requires four times the information bandwidth at S-band, but minimizes the number of S-band base stations to about 22 or 23.

The number of base stations can be increased, as the system traffic increases, without affecting the satellite antenna design. But the operational costs of these stations must be compared to the cost of the operational long distance land lines in order to determine the economical optimum.

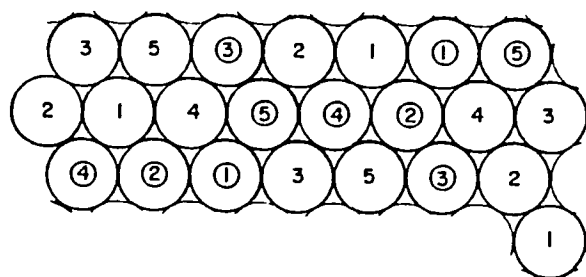
In principle, the required S-band beam topology can be implemented by using either the available UHF optics or separate optics.

For the common optics solution, the S-band feeds (horns or printed array sub-apertures) must be superimposed over the UHF feed clusters. This is feasible, provided the S-band and UHF component beam maximums do not coincide. However, for the common optics solution the following limitations apply:

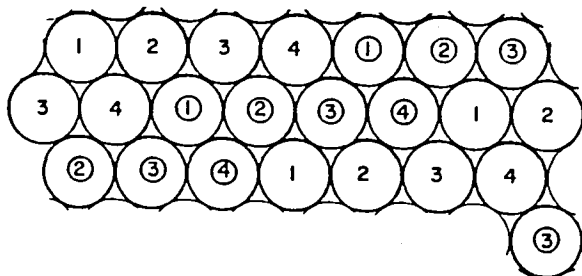
1. It is not practical to provide contiguous coverage in S-band. This seriously limits the system flexibility and particularly the increase of S-band base stations in the future.
2. The quality of the S-band beams is limited by the available surface accuracy of the quad aperture reflectors.
3. The quality of the UHF beams deteriorates in the presence of the S-band radiating elements. The restricted space means only certain (not necessarily optimum) type patch and BFN network layouts can be used in the UHF band.
4. The presence of S-band circuit components increases the thickness of the feed panels to the point that their packaging becomes impractical within the available volume.

Because of these limitations a separate S-band antenna was selected. The optics for this antenna is a single offset fed paraboloid, with a limitation on its diameter to allow it to be mounted behind the UHF feed cluster. In this manner, the design of the S-band antenna is completely separated from the UHF system, and its overall envelop stays well outside the main power flow of the lower frequency antenna.

Figure 7.1(a) shows a four frequency and figure 7.1(b) a five frequency beam topology plan using 22 beams. They allow, respectively, two or three empty cells between coverages.



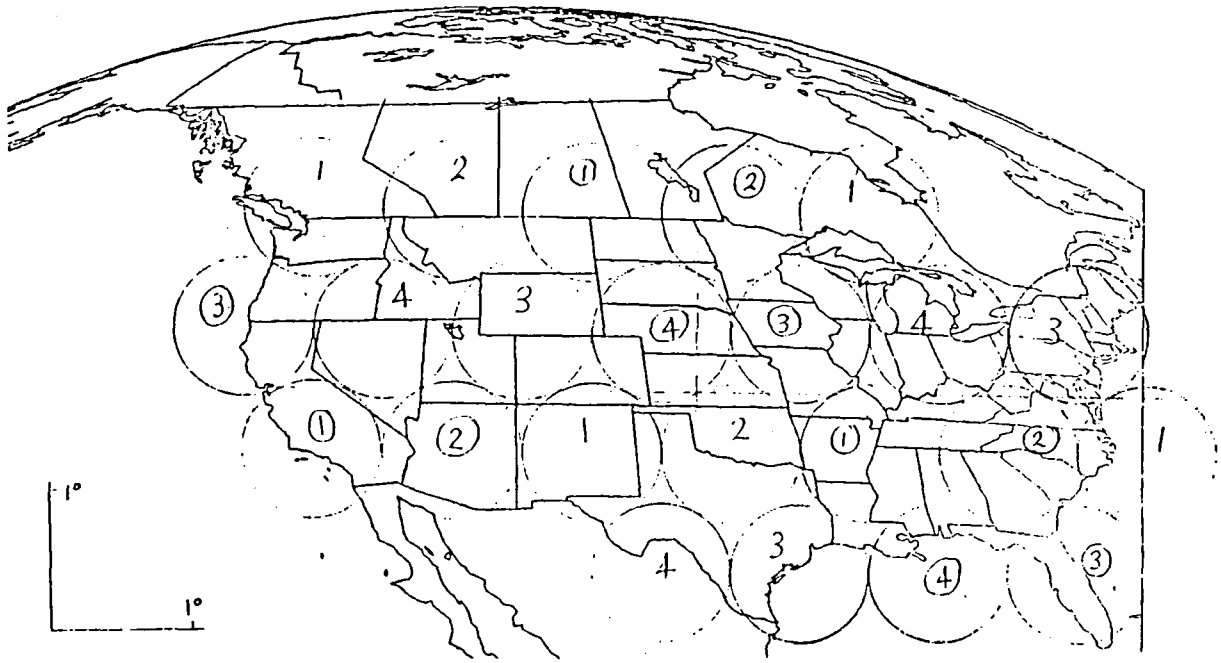
4 FREQUENCY PLAN,
2 EMPTY CELLS
n = 22



5 FREQUENCY PLAN,
3 EMPTY CELLS
n = 22

Figure 7.1.- S-band beam topology alternatives.

Figure 7.2 shows the selected S-band beam topology plan using 23 beams, $\alpha = 1^\circ$ cell sizes and a four frequency, dual polarization configuration.



SYNCHRONOUS VIEW AT -110.00 DEGREES LONGITUDE

Figure 7.2.- Selected S-band beam topology plan.

Figure 7.3 displays the superimposed UHF and S-band beam topology plans and the location of the S-band base stations (marked by heavy dots). The plan

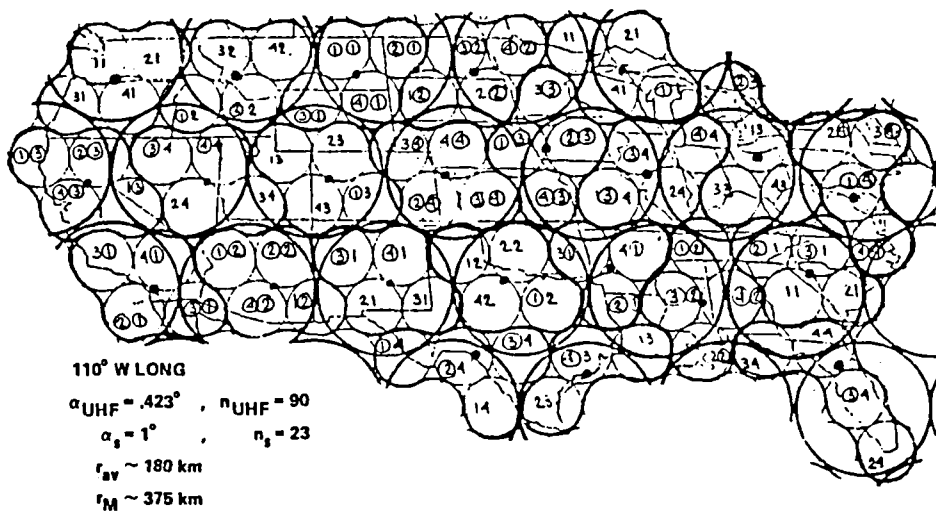


Figure 7.3.- Location of S-band base stations.

assures an average base station to fixed user distance of approximately 180 km and a maximum distance of approximately 375 km. The maximum distance can be reduced by about a factor of two at the expense of adding three more base stations and retaining the same spacecraft antenna diameter.

Figure 7.4 shows the profile of the reflector and feed of the S-band antenna. Waveguide type polarizer and horn is assumed for the radiating element.

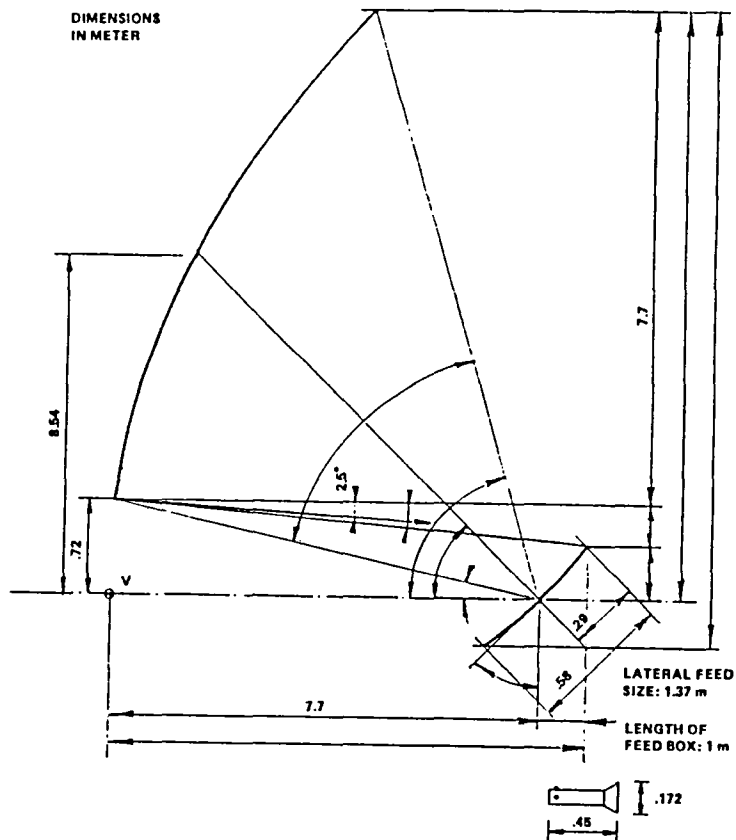
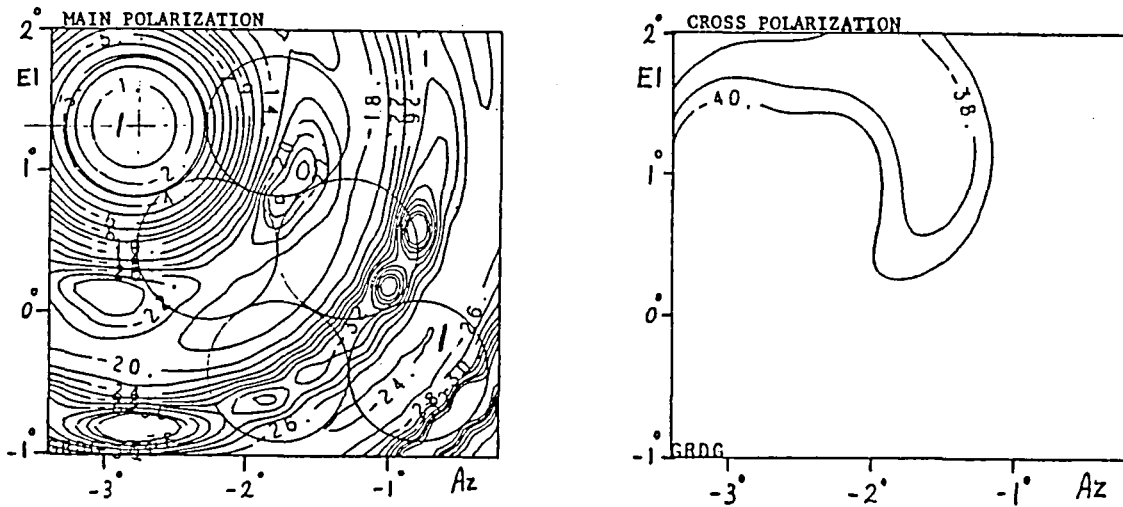
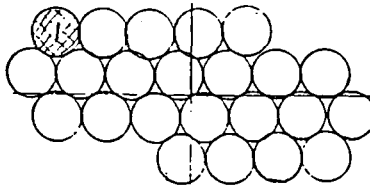


Figure 7.4.- Geometry of the S-band antenna.

Figure 7.5 shows the gain contour of the maximally scanned singlet beam using a TE_{11} mode excited circular aperture radiating element. Note that the sidelobe level is -24 dB and C/I is 21 dB in the applicable nearest interfered cell.



Configuration	TE ₁₁	S-Band 7m
Geometry	D, in	276.00
	F/D	1
	Q, in	19.2
	d, in	5.41
	α , deg	1.00
	n	1
Beam	-	N-WEST, FAR1



Polarization	R H C P
Longitude, deg.	110° W
Antenna Axis	EW
Pointing, Deg.	NS
EW Bias	
Frequency, GHz	2.62
Max. Gain, db	42.73

Figure 7.5.- Gain contour of the S-band antenna for a maximally scanned singlet.

Figure 7.6 shows the gain contour achieved by the use of a seven-element cluster. The maximum gain is 0.73 dB less than with a single element, but the sidelobe level is -35 dB and C/I is 33 dB in the interfered adjacent cell. The resultant C/I for the complete system is better than 27 dB.

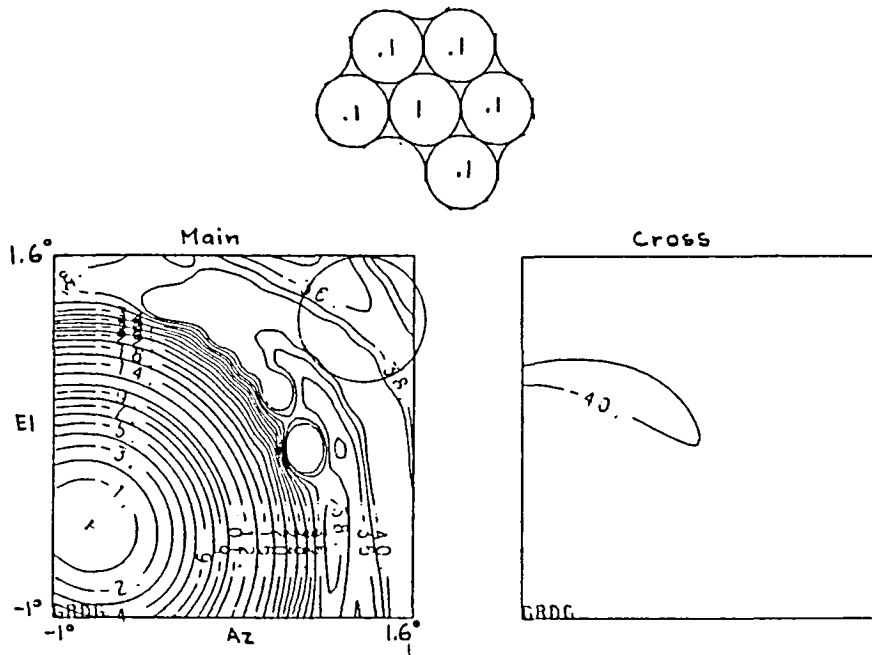


Figure 7.6.- Gain contour of the S-band antenna for a seven-element feed cluster.

On the basis of figures 7.5 and 7.6 it can be seen that depending on the system C/I requirement the one- or seven-element feed cluster per beam configuration can be selected. The optics and the feed cluster geometry are the same, but the second case requires a more complex beam forming network. Layout studies indicate that the feed - BFN - can be fitted in both cases within the available space.

In order to meet the overall packaging requirement a wrap-rib antenna was selected for the reflector structure of the offset fed paraboloid.

8. CONCLUSIONS AND RECOMMENDATIONS

- A single STS packaged 118 m diameter hoop column antenna is capable of providing service for approximately 250,000 mobile users.
- The selected quad aperture configuration is able to provide at least 25 dB C/I without the effect of cable blockage, column scatter, coupling between quad apertures, and tolerance effects.

- A feed can be designed which uses singular polarized radiating elements while the overall system employs dual polarization.
- The quad aperture concept can eliminate the use of diplexers and their associated losses.
- The control of beam isolation to protect from nearby, as well as remote "parasitic" sidelobes, requires an optimum layout of radiating elements, carefully selected excitation functions, and possibly the use of some parasitic radiation reducing shrouds. It is recommended that these effects are investigated further by using both analytical simulation and experimental techniques.
- The development of a proper printable radiating element (sub-array) plays a central role in the ultimate performance of the quad antenna for a mobile communication mission. Consequently, it is desirable to undertake the development of such a feed cluster at the earliest possible time.
- Tolerances in the mechanical implementation and BFN excitation areas result in major system limitations. These effects for a large deployable antenna, whether hoop column or wrap rib, are not fully understood. An early development of appropriate analytical techniques is necessary to derive the final specifications of an LMSS mission.

9. REFERENCES

1. Young, W. R., Advanced Mobile Phone Service: Introduction, Background, and Objectives. Bell System Technical Journal, Vol. 58, No. 1, January 1979, pp. 1-14.
2. Anderson, R. E., and Milton, R. T.: Satellite-Aided Mobile Radio Concepts Study: Concept Definition of a Satellite-Aided Mobile and Personal Radio Communication System. NASA CR-166646, June 1979.

1. Report No. NASA CR-3842		2. Government Accession No.		3. Recipient's Catalog No.	
4. Title and Subtitle RF CHARACTERISTICS OF THE HOOP COLUMN ANTENNA FOR THE LAND MOBILE SATELLITE SYSTEM MISSION				5. Report Date November 1984	
				6. Performing Organization Code	
7. Author(s) Peter Foldes				8. Performing Organization Report No.	
9. Performing Organization Name and Address Foldes Incorporated 1131 Radnor Hill Road Wayne, PA 19087				10. Work Unit No.	
				11. Contract or Grant No. NAS1-17209	
12. Sponsoring Agency Name and Address National Aeronautics and Space Administration Washington, DC 20546				13. Type of Report and Period Covered Contractor Report	
				14. Sponsoring Agency Code 506-62-43-01	
15. Supplementary Notes Langley Technical Monitor: Thomas G. Campbell Final Report					
16. Abstract This report describes a communication system using a satellite with a 118 meter diameter quad-aperture antenna to provide telephone service to mobile users remotely located from the large metropolitan areas where the telephone companies are presently implementing their cellular system. In this system, which is compatible with the cellular system, the mobile user communicates with the satellite at UHF frequencies (821-876 MHz). The satellite connects him at S-Band (2550-2690 MHz), to the existing telephone network via a base station. The report presents the results of the R.F. definition work for the quad-aperture antenna. The elements of the study requirements for the LMSS are summarized, followed by a beam topology plan which satisfies the mission requirements with a practical and realizable configuration. Based on this topology, the geometry of the UHF antenna and its radiation characteristics are defined. This is followed by a discussion of the various feed alternatives. Next, the S-Band aperture is described. Finally the report contains a conclusion and recommendation section.					
17. Key Words (Suggested by Author(s)) Land Mobile Satellite Cellular System Antenna, Parabolic Reflector Quad Aperture, Hoop/Column Feeds			18. Distribution Statement Unclassified - Unlimited Subject Category 32		
19. Security Classif. (of this report) Unclassified		20. Security Classif. (of this page) Unclassified		21. No. of Pages 65	22. Price A04

National Aeronautics and
Space Administration

Washington, D.C.
20546

Official Business
Penalty for Private Use, \$300

THIRD-CLASS BULK RATE

Postage and Fees Paid
National Aeronautics and
Space Administration
NASA-451



NASA

POSTMASTER: If Undeliverable (Section 158
Postal Manual) Do Not Return
